

The New Nuclide $^{263}_{105}\text{Ha}^{G,B}$

J.V. Kratz, M.K. Goyer, H.P. Zimmermann, Institut für Kernchemie, Universität Mainz
M. Schädel, W. Bröchle, E. Schimpf, GSI, Darmstadt

H. Gäggeler, D. Jost, J. Kovacs, U.W. Scherer, A. Weber, PSI, Villigen, Switzerland

K.E. Gregorich, A. Türler, B. Kadkhodayan, K.R. Czerwinski, N.J. Hannink, D.M. Lee, M.J. Nurmia,
D.C. Hoffman, Lawrence Berkeley Laboratory, Berkeley, California

In the course of a series of experiments investigating further the chemical properties [1] of element 105, hahnium, using the well-known isotope $34\text{-s } ^{263}_{105}\text{Ha}$ produced in the $^{249}\text{Bk} (^{18}\text{O},5n)$ reaction, we have developed and used a very efficient aqueous phase chemical separation procedure for hahnium: Ha^{5+} ions were complexed in 0.05 M α -hydroxy-iso-butyric acid (α -HIB) and eluted in $50 \mu\text{l}$ from $1.6 \times 8 \text{ mm}$ cation exchange columns. The effluent was quickly evaporated to dryness on Ta discs. Alpha and SF fragment pulse height analyses were performed on each sample using a system of ten 300 mm^2 passivated ion-implanted planar silicon detectors. Typical α -energy resolutions were 60 keV (FWHM). Each event was stored along with the time after start of counting and the detector identification. Start of counting was 40 s after the end of collection and the total counting time was 450 s.

The sum spectrum of all α -particle spectra containing α -events with $8.3 \leq E_{\alpha} \leq 8.7 \text{ MeV}$ obtained at 99 MeV bombarding energy is shown in Fig.1. Apart from a contamination by ^{249}Cf sputtered from the target (this material is not dissolved in the weakly acidic α -HIB solution and is washed mechanically through the column), and by a small Bi and Po activity produced by transfer reactions on a Pb impurity in the target, the spectrum is extremely clean and compatible with the complex spectra of ^{262}Ha and its daughter ^{268}Lr . Besides 41 α -events from ^{262}Ha and ^{268}Lr , among them 9 correlated pairs of parent-daughter decays with the correct half-life of $4.2^{+1.5}_{-1.1} \text{ s}$ for the correlated daughters, 23 fissions attributable to the decay of ^{262}Ha were also detected. These event rates are consistent with the detector efficiency and the known 5 n cross section [1] at 99 MeV.

Application of the same chemical separation-counting techniques to the products from a 93 MeV bombardment, chosen to optimize the production of the $4n$ reaction product, resulted in the α -spectrum shown in Fig.2. The absence of α -events above 8.5 MeV indicates that the $^{262}\text{Ha}/^{268}\text{Lr}$ couple is no longer present. We detected 9 α -particle decays with $8.3 \leq E_{\alpha} \leq 8.5 \text{ MeV}$ and 18 SF events that we attribute to the new isotope ^{263}Ha and its α -decay daughter, $6.4\text{-s } ^{269}\text{Lr}$ [2], produced in the $^{249}\text{Bk} (^{18}\text{O},4n)$ reaction with a cross section of $13 \pm 8 \text{ nb}$. The half-life for the new activity is 27^{+6}_{-5} s . The α -particle energy for ^{263}Ha is $8355 \pm 27 \text{ keV}$, that of ^{269}Lr is $8445 \pm 29 \text{ keV}$. Unfortunately, we did not observe pairs of correlated mother-daughter α -particles, however, two α -SF correlations with correlation times of 6.0 and 8.58 s were observed, compatible with the 23% SF branch [2] in ^{269}Lr . The frequency at which various event types associated with the decay of $^{263}\text{Ha}/^{269}\text{Lr}$ were observed, is consistent with the detection

efficiency and with a SF branch in ^{263}Ha of $57^{+13}_{-15}\%$.

The kinetic energy distribution of the 18 SF events suggests that the average kinetic energy is 207 MeV, and the distribution is probably symmetric. Both the value of $\langle \text{TKE} \rangle$ and the apparent symmetry of the distribution are consistent with SF systematics [3].

- [1] J.V. Kratz et al., *Radiochim. Acta*, **48**, 121 (1989)
- [2] K.E. Gregorich, private communication
- [3] D.C. Hoffman, *Nucl.Phys.* **A502**, 21c (1989)

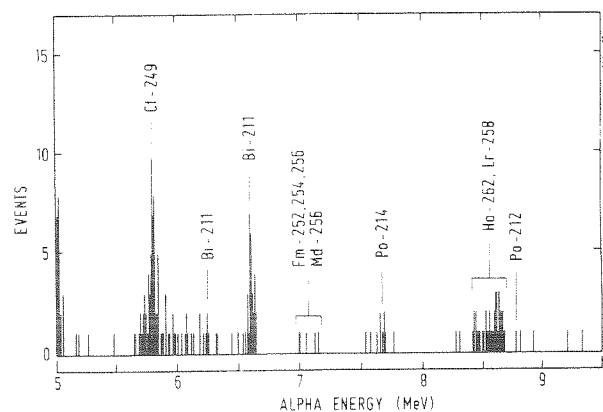


Fig.1 Sum spectrum of all α -particle spectra containing events with $8.3 \leq E_{\alpha} \leq 8.7 \text{ MeV}$ in the bombardment of ^{249}Bk with $22.3 \mu\text{Ah}$ of 99 MeV $^{18}\text{O}^{5+}$ ions after cation exchange separations in 0.05 M α -HIB.

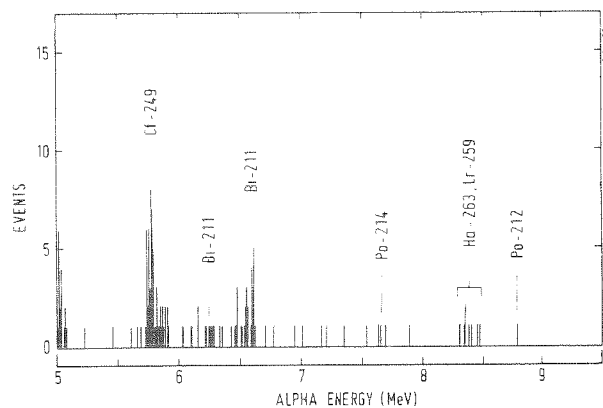


Fig.2 Sum spectrum of all α -particle spectra containing events with $8.3 \leq E_{\alpha} \leq 8.7 \text{ MeV}$ in the bombardment of ^{249}Bk with $15.6 \mu\text{Ah}$ of 93 MeV $^{18}\text{O}^{5+}$ ions. The chemical procedure was the same as for Fig.1.

The New Nuclide $^{263}_{105}\text{Ha}^{G,B}$

J.V. Kratz, M.K. Gober, H.P. Zimmermann, Institut für Kernchemie, Universität Mainz
M. Schädel, W. Bröchle, E. Schimpf, GSI, Darmstadt

H. Gäggeler, D. Jost, J. Kovacs, U.W. Scherer, A. Weber, PSI, Villigen, Switzerland

K.E. Gregorich, A. Türler, B. Kadkhodayan, K.R. Czerwinski, N.J. Hannink, D.M. Lee, M.J. Nurmia,
D.C. Hoffman, Lawrence Berkeley Laboratory, Berkeley, California

In the course of a series of experiments investigating further the chemical properties [1] of element 105, hahnium, using the well-known isotope $34\text{-s } ^{263}_{105}\text{Ha}$ produced in the $^{249}\text{Bk} (^{18}\text{O},5n)$ reaction, we have developed and used a very efficient aqueous phase chemical separation procedure for hahnium: Ha^{5+} ions were complexed in 0.05 M α -hydroxy-iso-butyric acid (α -HIB) and eluted in $50 \mu\text{l}$ from $1.6 \times 8 \text{ mm}$ cation exchange columns. The effluent was quickly evaporated to dryness on Ta discs. Alpha and SF fragment pulse height analyses were performed on each sample using a system of ten 300 mm^2 passivated ion-implanted planar silicon detectors. Typical α -energy resolutions were 60 keV (FWHM). Each event was stored along with the time after start of counting and the detector identification. Start of counting was 40 s after the end of collection and the total counting time was 450 s.

The sum spectrum of all α -particle spectra containing α -events with $8.3 \leq E_{\alpha} \leq 8.7 \text{ MeV}$ obtained at 99 MeV bombarding energy is shown in Fig.1. Apart from a contamination by ^{249}Cf sputtered from the target (this material is not dissolved in the weakly acidic α -HIB solution and is washed mechanically through the column), and by a small Bi and Po activity produced by transfer reactions on a Pb impurity in the target, the spectrum is extremely clean and compatible with the complex spectra of ^{262}Ha and its daughter ^{268}Lr . Besides 41 α -events from ^{262}Ha and ^{268}Lr , among them 9 correlated pairs of parent-daughter decays with the correct half-life of $4.2^{+1.5}_{-1.1} \text{ s}$ for the correlated daughters, 23 fissions attributable to the decay of ^{262}Ha were also detected. These event rates are consistent with the detector efficiency and the known 5 n cross section [1] at 99 MeV.

Application of the same chemical separation-counting techniques to the products from a 93 MeV bombardment, chosen to optimize the production of the $4n$ reaction product, resulted in the α -spectrum shown in Fig.2. The absence of α -events above 8.5 MeV indicates that the $^{262}\text{Ha}/^{268}\text{Lr}$ couple is no longer present. We detected 9 α -particle decays with $8.3 \leq E_{\alpha} \leq 8.5 \text{ MeV}$ and 18 SF events that we attribute to the new isotope ^{263}Ha and its α -decay daughter, $6.4\text{-s } ^{269}\text{Lr}$ [2], produced in the $^{249}\text{Bk} (^{18}\text{O},4n)$ reaction with a cross section of $13 \pm 8 \text{ nb}$. The half-life for the new activity is 27^{+6}_{-5} s . The α -particle energy for ^{263}Ha is $8355 \pm 27 \text{ keV}$, that of ^{269}Lr is $8445 \pm 29 \text{ keV}$. Unfortunately, we did not observe pairs of correlated mother-daughter α -particles, however, two α -SF correlations with correlation times of 6.0 and 8.58 s were observed, compatible with the 23% SF branch [2] in ^{269}Lr . The frequency at which various event types associated with the decay of $^{263}\text{Ha}/^{269}\text{Lr}$ were observed, is consistent with the detection

efficiency and with a SF branch in ^{263}Ha of $57^{+13}_{-15}\%$.

The kinetic energy distribution of the 18 SF events suggests that the average kinetic energy is 207 MeV, and the distribution is probably symmetric. Both the value of $\langle \text{TKE} \rangle$ and the apparent symmetry of the distribution are consistent with SF systematics [3].

- [1] J.V. Kratz et al., *Radiochim. Acta*, **48**, 121 (1989)
- [2] K.E. Gregorich, private communication
- [3] D.C. Hoffman, *Nucl.Phys.* **A502**, 21c (1989)

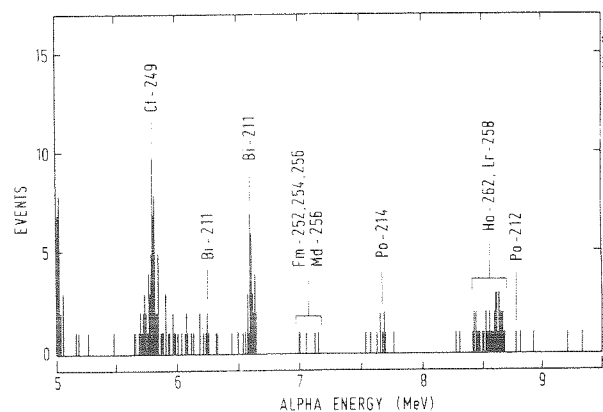


Fig.1 Sum spectrum of all α -particle spectra containing events with $8.3 \leq E_{\alpha} \leq 8.7 \text{ MeV}$ in the bombardment of ^{249}Bk with $22.3 \mu\text{Ah}$ of 99 MeV $^{18}\text{O}^{5+}$ ions after cation exchange separations in 0.05 M α -HIB.

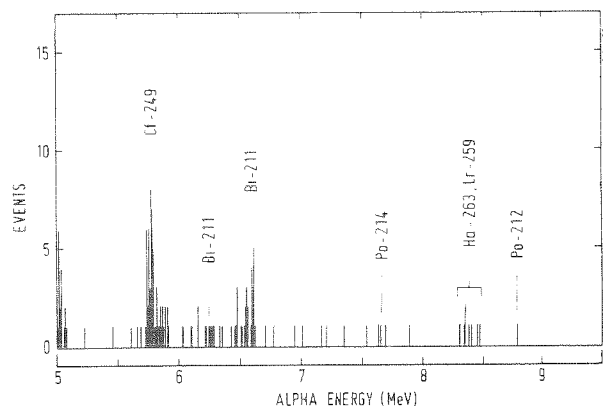


Fig.2 Sum spectrum of all α -particle spectra containing events with $8.3 \leq E_{\alpha} \leq 8.7 \text{ MeV}$ in the bombardment of ^{249}Bk with $15.6 \mu\text{Ah}$ of 93 MeV $^{18}\text{O}^{5+}$ ions. The chemical procedure was the same as for Fig.1.

Surprisingly High Cross Section for $^{263}_{105}\text{Ha}$ ^{G, B}

M. Schädel, W. Bröchle, E. Schimpf

GSI Darmstadt

J.V. Kratz, H.P. Zimmermann, M.K. Goyer

Institut für Kernchemie, Universität Mainz

H. Gäggeler, D. Jost, J. Kovacz, U.W. Scherer, A. Weber

Paul Scherrer Institut, Villigen

K.E. Gregorich, A. Türrier, B. Kadkhodayan, K.R. Czerwinski, N.J. Hannink, D.M. Lee, D.C. Hoffman

Lawrence Berkeley Laboratory, Berkeley

In a series of experiments investigating the chemical properties of element 105, hahnium, we have observed a new alpha and SF activity that we assign to the new isotope $^{263}_{105}\text{Ha}$; see Ref.1 for a more detailed description of the experiment, the decay characteristics of this isotope, and the grounds on which our assignment is based. The new isotope ^{263}Ha has been produced in a $^{249}\text{Bk}(^{18}\text{O},4n)$ reaction with a cross section of 13 ± 8 nb at 93 MeV bombarding energy. The large error results from a conservative estimate of the uncertainties of the chemical yield and the gas jet transport efficiency. At 93 MeV no contribution from ^{262}Ha has been observed, and an upper limit cross section of 1.3 nb can be estimated for this 5n-product (assuming zero events observed corresponding to 3 events at 95% confidence level).

The cross section for production of ^{262}Ha at 99 MeV as reported earlier² must be revised because both isotopes, ^{262}Ha and ^{263}Ha , are produced at this energy. Because of the very similar decay characteristic of both isotopes the contribution from ^{263}Ha has so far been assigned to ^{262}Ha resulting in a too large cross section of ^{262}Ha . From our recent experiments¹ we conclude that the new cross sections at 99 MeV are 6 ± 3 nb for ^{262}Ha , and 2 ± 1 nb for ^{263}Ha , respectively.

As these isotopes belong to the most neutron-rich isotopes which can only be produced in so called hot fusion reactions based on actinide targets their production cross section is of interest for extrapolations into the yet unknown region of deformed nuclei with enhanced shell stabilization around $Z = 109$ and $N = 162^3$. One empirical approach to make such extrapolations is to plot measured cross sections vs atomic number.

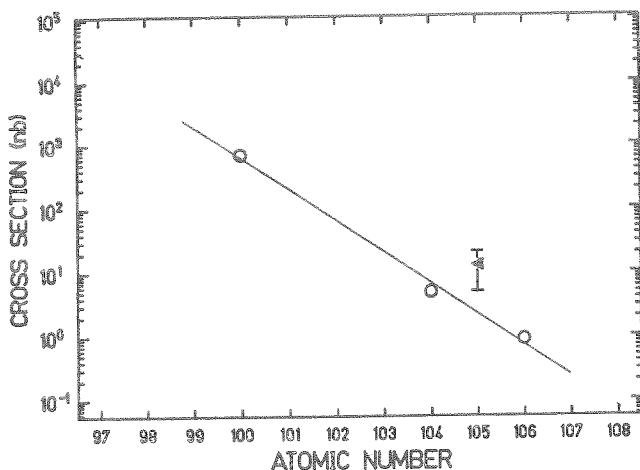


Fig.1: Correlation for ($^{18}\text{O},4n$) reaction cross sections.

Fig. 1 shows the correlation for ^{18}O induced reactions to produce the heavy element isotopes $^{252}\text{Fm}^4$, $^{262}_{104}\text{Sg}^5$ and $^{263}_{105}\text{Ha}^6$ (open circles). The new isotope ^{263}Ha (triangle) has a cross section significantly higher than expected.

A more elaborated but to some extent still empirical approach is the use of a fusion-evaporation code. It has been shown that HIVAP provides an excellent description of isotope production of the heaviest element isotopes in hot fusion reactions⁷. Not only the position of the maxima of the excitation functions has been reproduced by the calculations but also up to element 106, calculation and experiment agreed within a factor of 2 regarding the absolute cross section values. It is evident from Fig. 2 that the measured cross section of the new isotope ^{263}Ha is significantly higher than expected from the calculations. For this calculation the same set of parameters has been used as in the previous, successful description of experimental data⁷. At the moment it is premature to present any explanation for the high cross section. One may speculate to see a first indication for enhanced nuclear stability towards heavier, more neutron-rich isotopes. Increasing shell effects³ may lead to an increase in the survival probability during the deexcitation of the compound nucleus.

1. J.V. Kratz et al., contribution to this report
2. J.V. Kratz et al., Radiochim. Acta 48, 121 (1989)
3. K. Böning et al., Z. Phys. A325, 479 (1986)
4. T.Sikkeland Ark. Fys. 36, 539 (1966)
5. L.P. Somerville et al., Phys. Rev. C31, 1801 (1985)
6. V.A. Drulin et al., Sov. J. Nucl. Phys. 25, 591 (1979)
7. M. Schädel, GSI Scientific Report 1988, GSI 89-1, p.19

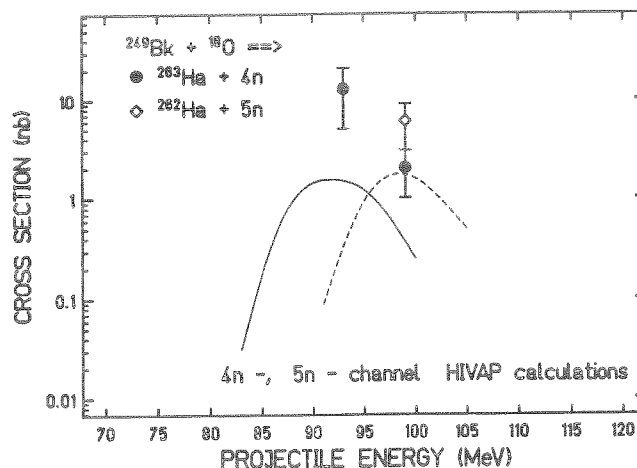


Fig.2: Comparison of calculated and measured cross sections.

Search for Supermassive Nuclei in Nature ^B

S.Polikanov¹, C.S.Sastri¹, G.Herrmann², K.Lützenkirchen², M.Overbeck², N.Trautmann², A.Breskin³, R.Chechik³, Z.Fraenkel³

¹Gesellschaft für Schwerionenforschung, Darmstadt

²Institut für Kernchemie der Universität Mainz

³Weizmann Institute of Science, Rehovot, Israel

We report on a search for supermassive nuclei in nature with masses up to 10^7 amu. Such exotic nuclei might consist, for example, of stable strange matter [1], which comprises a mixture of up, down, and strange quarks, or of relic particles [2] from the early Universe. The experiments are based on Rutherford backscattering of heavy ions, preferably ^{238}U , from various target samples.

In a previous note [3] we reported on the results of a search for supermassive nuclei in iron meteorites and some terrestrial samples. No indication for the presence of supermassive isotopes was observed. In order to improve the experimental limits we examined additional meteorite targets and prepared a target sample chemically enriched in strange-matter content.

The most efficient way of obtaining an enriched sample is to use a target composed of unstable elements (e.g. transuranic elements). In this case, strange matter can be chemically extracted from a large amount of bulk material that contains or did contain unstable elements. We investigated the backscattering of uranium nuclei by a target which was prepared from the plutonium fraction of a chemical extraction starting from an initial mineral sample of 85 kg [4].

Another type of samples that are of interest to investigate are the carbonaceous chondrites (Orgueil-, Murchison-, Allende-meteorite). In the course of their history they have not been subjected to gravitational effects so that no chemical fractionation due to the difference in masses occurred.

The experiments were carried out with a beam of ^{238}U at an energy of 1.4 MeV/u. The signature of supermassive nuclei would be the observation of heavy ions scattered into the backward hemisphere without essential loss of energy. The experimental set-up is described in Refs. [3] and [5]. It consists of twelve position-sensitive multi-wire proportional counters divided into four start- and eight stop-detectors. For each scattered ion we measured the scattering angle, the time-of-flight (TOF), and the specific ionization (ΔE) produced in the stop-counter.

In Fig.1 we show the two-dimensional spectrum of ΔE against TOF for the plutonium sample; the spectrum was measured in the angular range 92° - 118° . A number of nuclei is registered with ΔE below that of uranium and with TOF ≈ 30 - 90 ns. These events result from backward rescattering of recoil nuclei produced in collisions of uranium with nuclei of lighter elements in the target. For TOF ≥ 90 ns there are some events with ΔE of uranium nuclei. They most likely stem from ^{238}U nuclei emitted into the backward hemisphere by multiple scattering; these events were excluded from the further analysis. A TOF of 90 ns corresponds to backscattering of uranium nuclei from target nuclei with mass $A = 400$ located on the target surface. Thus, by excluding the events with TOF ≥ 90 ns, we confine ourselves to a mass range of supermassive nuclei with the lower limit $A = 400$.

In Fig.1 we can see an event (marked with A) with TOF = 60 ns and a ΔE within the 2σ -range from the centroid of uranium nuclei as determined in a calibration experiment. The proba-

bility that the event (A) is a uranium nucleus is 14%. On the other hand, the event could also be a multiply scattered light target nucleus with exceptionally high ΔE . The ΔE -spectra in calibration experiments indeed have a high-energy tail which is most likely caused by random coincidences [4]. Thus, using Poisson statistics, the probability that (A) is a light target nucleus is found to be 9%.

Upon irradiation of the meteorite targets no backscattered ^{238}U was recorded with TOF ≤ 90 ns, and thus our data can be used only for an estimate of the upper limit of the abundance of strange matter. The resulting limits [4] for the abundance of strange nuggets with masses $A \approx 4 \cdot 10^3$ to 10^7 amu relative to the number of nucleons are ranging from $6 \cdot 10^{-12}$ to $3 \cdot 10^{-16}$ for the meteorite targets. For the chemically enriched plutonium sample the respective limit of $2 \cdot 10^{-17}$ is valid for strange matter of positive charge $Z=94$, which corresponds to a mass of $A \approx 3700$ [1].

Our previous limit [3] for the abundance of strange matter was close to an estimate by De Rújula and Glashow [6] who assumed that the local dark matter density of our Galaxy consists of strange nuggets. In the present study the upper limit is about three orders of magnitude below their estimated abundance of strange matter.

References:

- [1] E. Farhi, R.L. Jaffe, Phys. Rev D30, 2379 (1984)
- [2] J. Ellis et al., Nucl. Phys. B177, 427 (1981)
- [3] M. Brügger et al., Nature 337, 434 (1989)
- [4] S. Polikanov et al., Z. Phys. A, in press
- [5] M. Overbeck et al., Nucl. Instr. Meth. A288, 413 (1990)
- [6] A. De Rújula, S.L. Glashow, Nature 312, 734 (1984)

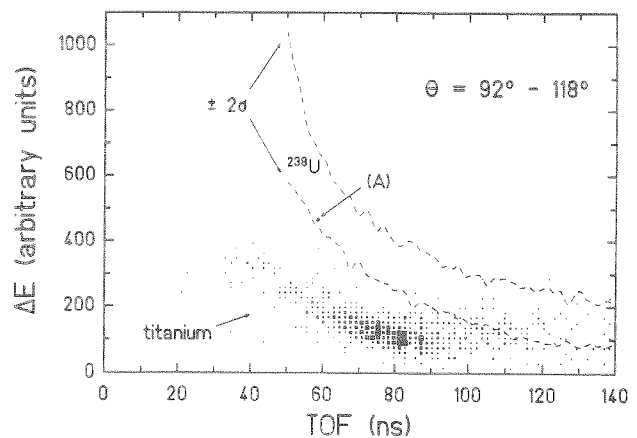


Figure 1 : ^{238}U ions incident on a target prepared from a plutonium fraction; two-dimensional spectrum of ΔE against TOF in the angular region 92° - 118° .

Excitation - Energy Sharing in the Reaction $^{51}\text{V} + ^{197}\text{Au}$ at the Barrier ^B

P. Klein¹, W. Bruechle², M. Guber¹, J.V. Kratz¹, M. Schädel², P. Zimmermann¹

¹ Institut für Kernchemie, Universität Mainz

² GSI, Darmstadt

The excitation - energy sharing among the reaction products contains important information about the intrinsic equilibration process in heavy - ion collisions. Deviations from thermal equilibrium with an excitation - energy division proportional to the ratio of the fragment masses have been observed repeatedly, in particular for the early equilibration phase. Also, for low dissipated energies, an extreme dependence of the excitation - energy division on the direction of the mass flow was observed¹. For quasi - fission reactions characterized by the complete damping of the kinetic energy and by large mass and charge transfer, one might expect that thermal equilibrium is reached. However, we have previously^{2,3} observed cold target - like fragments and highly excited projectile - like fragments in quasi - fission reactions at the barrier. The suggested mechanism is a highly ordered transfer of nucleons from the outermost orbitals of the target to unoccupied orbitals in the projectile leaving a cold core of the target nucleus and producing an excited projectile - like acceptor with as many particle - hole excitations as particles were transferred. The absence of equilibration may be associated with the initial absence of a friction force because the experiments were performed exactly at the Coulomb barrier where the relative velocity is zero.

An alternative interpretation⁴ assumes that nucleon transfer is a random process populating single - particle states both in the target - and projectile - like nucleus near the Fermi energy. This would always make, at low energies, the lighter nucleus more highly excited than the heavier nucleus. A dependence of the energy sharing on the direction of the mass flow is then not to be expected.

Our previous experiments^{2,3} were restricted to observing the mass flow from the target to the projectile. In order to test a possible dependence of the excitation - energy division on the direction of the mass flow we looked also at the below - projectile and trans - target products in the reaction $^{51}\text{V} + ^{197}\text{Au}$ at the Coulomb barrier ($E_{\text{Lab}} = 248 \text{ MeV}$). The reaction products, after being stopped in 4π geometry in catcher foils, were subject to extensive chemical separations⁵ and low - level γ - ray spectroscopy over a period of several weeks. The resulting cross sections are used to define centroids $\langle N \rangle_Z$ of the isotope distribution for given elements. These post - neutron emission centroids are compared with pre - neutron emission centroids calculated by using the minimum potential energy (MPE) concept. The resulting missing mass will be used to determine the average excitation energy as a function of Z with the help of evaporation calculations.

Figs. 1 and 2 depict the locations of the experimental centroids $\langle N \rangle_Z$ in the $N - Z$ plane overlaid by the potential energy surface. The following observations can be made: The centroids for the above - projectile products (acceptors) are all shifted to the left hand side from the MPE - line by the evaporation of about 4 neutrons, i.e. the acceptors have been excited. The centroids for the below - projectile products coincide with the MPE - line, i.e. the donors stayed cold and did not evaporate particles. Consistently,

below the target, we observe centroids close to the MPE - line, and centroids crossing the MPE - line to the left hand side above the target. Thus, the preliminary results point to a dependence of the excitation - energy sharing on the direction of the mass flow.

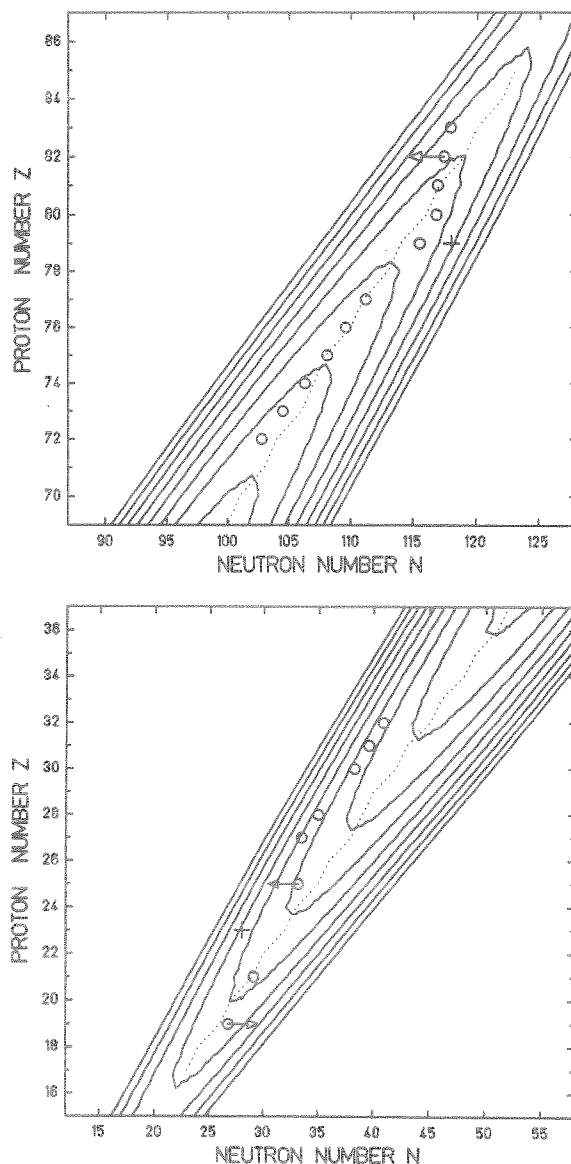


Fig.1,2: Calculated potential energy surface (PES) for $^{51}\text{V} + ^{197}\text{Au}$ ($l = 7\hbar$, $R_{\text{min}} = 13.4 \text{ fm}$). Shown are equipotential lines with 3 MeV spacing. The minimum potential energy (MPE) is indicated by the dotted line. Circles (o) mark the position of the centroids of the isotope distribution for given values of Z , the injection points are depicted with +.

¹H. Sohlbach et al., Phys. Lett. **153B**, 386 (1985)

²H. Keller et al., Z. Phys. **A328**, 255 (1987)

³H. Gaggeler et al., Phys. Rev. **C33**, 1983 (1986)

⁴G. Beier et al., Z. Phys. **A336**, 217 (1990)

⁵P. Klein, Diplomarbeit (1989)

Model Experiments for Separations of Elements 104 and 105

H. Bruchertseifer, W. Heller
 Zentralinstitut für Isotopen- und Strahlenforschung, Leipzig
 F. Haberberger, N. Trautmann, P. Zimmermann
 Institut für Kernchemie, Universität Mainz
 M. Schädel, W. Brüche
 GSI Darmstadt
 G. Skarnemark
 Chalmers University of Technology, Göteborg
 O. Alstad
 Department of Chemistry, University of Oslo
 V.P. Domanov, Z. Szegłowski, M. Vobecky
 Joint Institute for Nuclear Research, Dubna

To develop a separation procedure for the elements 104 and 105 the lighter homologs Zr and Nb as well as Hf and Ta have been used as tracers.

The difference in complex formation of Zr and Nb in aqueous hydrofluoric acid solutions has been applied for their separation. Zr forms cationic complexes in diluted hydrofluoric acid, which can be adsorbed on a cation exchange resin while the negative charged niobium complexes remain in the solution. To find out optimum separation conditions experiments have been performed with fission products at the TRIGA Mainz combined with the centrifuge system SISAK III¹. The fission products are transported from the irradiation position to the SISAK system with a KCl/N₂ gas jet. The clusters with the attached products are dissolved in 0.1 M HCl and HF of different concentrations in a degasser where the nobel gases together with the jet gas are removed. The outgoing solution is passed with a flow rate of 20 ml/min through the 30 x 3 mm² cation exchange column filled with 100 - 200 mesh DOWEX 50 x 8. The effluent is pumped to the HP-Germanium detector and is measured.

Fig. 1 shows part of a gamma ray spectrum of the fission product activities in this effluent (upper part without and lower part after a separation step). After introducing a DOWEX 50 column for separation the strongest γ -lines of ⁹⁹Nb and ¹⁰¹Nb can clearly be seen whereas the Zr-lines have disappeared indicating that the Zr and the lanthanides are adsorbed at the column.

The results of the experiments with different HF concentrations are summarised in table 1.

Tab. 1: Percentages of the initial Zr activity present in the Nb fraction measured as a function of the HF concentration

M / HF	%
1 x 10 ⁻³	≤4.6
5 x 10 ⁻⁴	≤2.3
1 x 10 ⁻⁴	6.6
1 x 10 ⁻⁵	8.5
without separation	100 (defined)

From this data one can see that in 0.1 M HCl containing HF concentrations between 10⁻³ and 10⁻⁵ mol/l Nb forms anionic fluoride complexes. At low HF concentrations (< 5 x 10⁻⁴ M) Nb begins to form partly neutral and cationic complexes leading

to a decrease of the Nb-activity in the effluent. This separation method for Nb and Zr should also be applicable for the elements 105 and 104 if the behaviour of these elements is similar to the lighter elements in the 5th subgroup. With this chemical procedure it is also possible to separate fast and continuously both elements from the actinides². Differences in the adsorption with varying HF concentrations could give informations about the complex formation of the element 105 with F⁻ and OH⁻ ions.

1. H. Persson et al., Radiochim. Acta 48, 177 (1989)
2. Z. Szegłowski et al., Radiochim. Acta 51, 71 (1990)

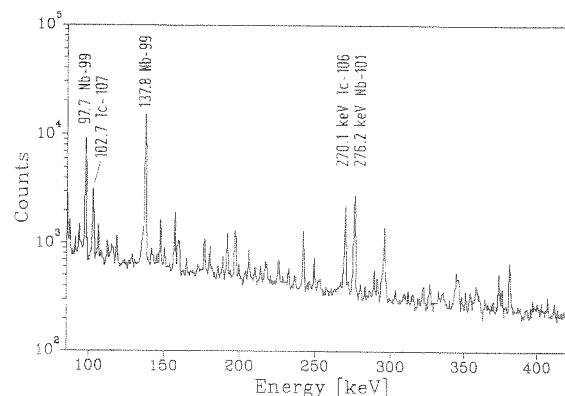
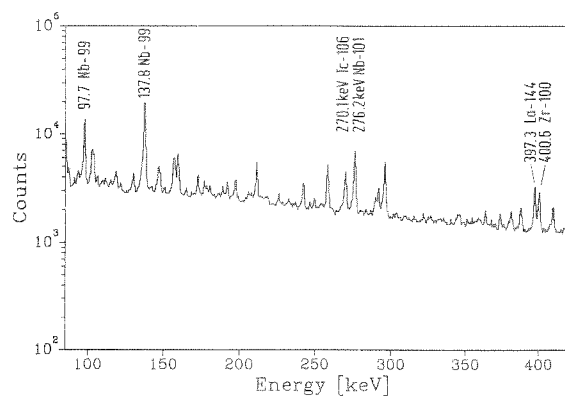


Fig.1: Parts of γ -spectra from the solution without (upper part) and with (lower part) separation

Development of a Chemical Separation Procedure for Element 106

W. Heller, H. Bruchertseifer (Zentralinstitut für Isotopen- und Strahlenforschung, Leipzig)

F. Haberberger, N. Trautmann (Institut für Kernchemie, Universität Mainz)

M. Schädel (GSI Darmstadt)

G. Skarnemark (Chalmers University of Technology, Göteborg)

O. Alstad (Department of Chemistry, University of Oslo)

Fast and continuous chemical techniques for element 106 from complex reaction products can be tested with fission products assuming that the behaviour of element 106 is similar to the lighter homolog of the 6th subgroup, molybdenum. Experiments have been performed at the TRIGA Mainz to check the possibility of separating molybdenum from niobium (5th subgroup), zirconium (4th subgroup), and the lanthanides (3rd subgroup) in alkaline solution.

The fission products, produced by thermal neutron induced fission of ²³⁹Pu, were transported by a KCl/N₂ gas jet to the dissolution-degasser unit of the centrifuge system SISAK III'. The clusters with the attached fission products were dissolved in a aqueous solution of NaOH or NH₃. After removing the nobel gases and the carrier gas the solution was pumped with a flow rate of 31 ml/min through a filter with thin layers of Nb(OH)₅ and La(OH)₃ precipitates and through a 30 x 3 mm² column filled with the cation exchange resin 100 - 200 mesh DOWEX 50 x 8. This separation was performed in analogy to the one described in Ref.2. The effluent was transported through a teflon tube to a HP-Germanium detector and was measured (see fig. 1 for a schematic of the experimental set-up).

The variation of the pH-value of the solution and the use of different layers of hydroxid precipitates on the filter led to results given in tab. 1.

Tab. 1: Results of separations of Mo as a model element for element 106 from La and Nb under different conditions with a cation exchange column

solution	pH	filter	ratio of peak areas from main γ -energies in solution with and without separation		
			¹⁰⁵ Mo	¹⁴⁴ La	⁹⁹ Nb
NH ₃	11.3	-	64.2%	11.3%	38.7%
NaOH	12.0	Nb(OH) ₅ La(OH) ₃	94.8%	9.5%	2.4%
NaOH	13.0	Nb(OH) ₅ La(OH) ₃	100%	<3%	<4%

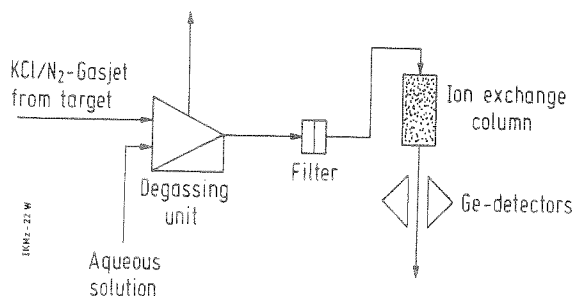


Fig.1: Experimental set-up

One can see that the optimum conditions for the separation of Mo were obtained from a solution of NaOH (pH = 13), in combination with Nb(OH)₅ and La(OH)₃ on a set of glasfibre and membrane filters.

Fig. 2 shows part of the γ -ray spectrum of the solution without (upper part) and with (lower part) separation in the energy range from 120 to 315 keV. After the separation only the peaks from ¹⁰⁵Mo and ¹⁰⁶Tc can be seen, whereas peaks of niobium (⁹⁹Nb, ¹⁰¹Nb and ¹⁰²Nb), zirconium (¹⁰²Zr), and lanthanum (¹⁴⁴La) have completely disappeared, which indicated that all these elements are adsorbed at the cation exchange column and the filters with the precipitates.

Further experiments are planned to optimize the separation technique and extend the procedure to tungsten.

1. H. Persson et al., Radiochim. Acta 48, 177 (1989)
2. H. Bruchertseifer et al., Radiochim. Acta 47, 41 (1989)

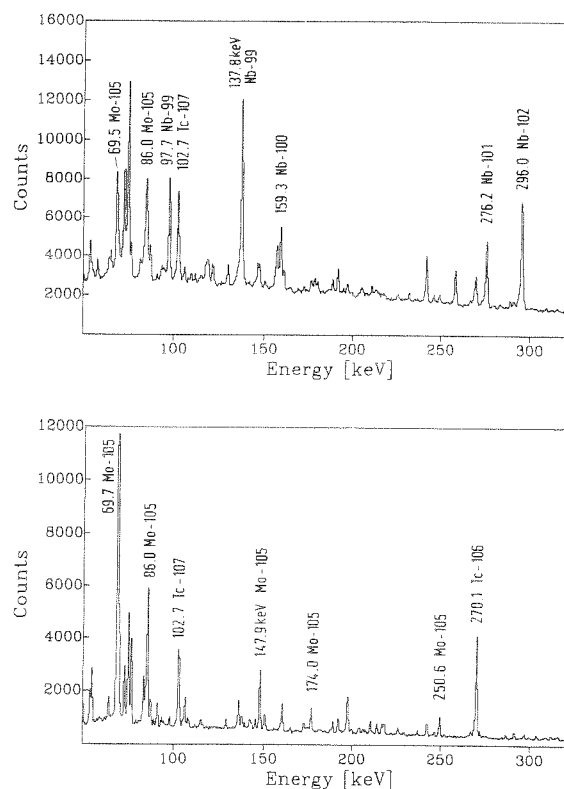


Fig.2: Part of γ -ray spectrum of the solution without (upper part) and with (lower part) separation

A PROPOSED SEPARATION SCHEME FOR THE SEPARATION OF LEAD FROM LORANDITE

W. Bröchle, B. Schausten, GSI Darmstadt, FRG

LOREX is a project to use thallium as a geological solar-neutrino detector /1/. Lorandite (TlAsS_2) is the only known Tl mineral which could be used to detect ^{205}Pb produced by solar neutrinos from ^{205}Tl . Some prerequisites for such a mineral are: it must contain very low levels of lead (≈ 1 ppm typically for Lorandite), and the "irradiation age" must be known. The latter is important because reactions with cosmic radiations can lead to ^{205}Pb , too. The main problem is, that only 30-100 atoms of ^{205}Pb are estimated to be formed by neutrinos in 1g of Lorandite during the geological age of the deposit ($\approx 5 \times 10^6$ a) /2/. Compared to 1.2×10^{21} atoms of ^{205}Tl in the same sample, this yields a surplus of a factor of $\approx 2 \times 10^{19}$ for ^{205}Tl .

If we assume that the detection of ^{205}Pb shall be done by accelerator mass spectroscopy (AMS) /3/ we can estimate the amount of Lorandite needed, and the chemical separation factors required before mass separation. AMS yields isobar separations $^{205}\text{Pb}:^{205}\text{Tl}$ of $\approx 1:10^3$. A negative ion sputter source /4/ can yield ionisation efficiencies $\text{Pb:Tl} \approx 1:10^2$. A combination of AMS with this ion source would allow 1 atom of ^{205}Pb to be detected in 10^5 atoms of ^{205}Tl . The chemical purification should then yield separation factors Pb:Tl better than $1:10^{15}$. The absolute efficiency of AMS nowadays is less than 10^{-4} . To detect at least 100 atoms of ^{205}Pb (statistical error $1\sigma = 10\%$) one needs $\geq 10\text{Kg}$ Lorandite. This amount is needed independently from different levels of the Allchar deposit in order to correct for myon- induced reactions from cosmic radiation. Nowadays only $\approx 50\text{g}$ of Lorandite exist concentrated and separated out of the surrounding minerals from the Allchar deposit.

The problem of contaminating the samples with lead from aerosols (leaded fuels) should not be underestimated. The content of ^{205}Pb in natural lead is not known. But with the measured thermal neutron flux from the Allchar mine /5/ of $4.4 \times 10^{-3} \text{ cm}^{-2}\text{s}^{-1}$ at the surface and the known cross section for the reaction $^{204}\text{Pb}(n,\gamma)^{205}\text{Pb}$ one can calculate a content of 3×10^{-14} ^{205}Pb in natural Pb at the earth surface. This may be only a lower limit because reactions with high energetic cosmic radiations were ignored. This means, that 10mg Pb which should be in 10Kg of Lorandite could contain 9×10^5 atoms of ^{205}Pb , the same amount which optimistically is expected from neutrino reaction with Tl.

We evaluated a separation scheme which shall overcome the separation problems. All experiments were done with β -decaying tracer activities of ^{204}Tl ($T_{1/2} = 3.78\text{a}$) and ^{212}Pb ($T_{1/2} = 10.64\text{h}$) which were measured in a low level proportional counter. ^{212}Pb could be measured with better sensitivity via its α -decaying daughter ^{212}Bi ($T_{1/2} = 60.6\text{m}$) using surface- barrier Si-detectors.

In a first step the Lorandite which is not soluble in HCl should be washed with dilute hydrochloric acid to remove possible surface contaminations from lead which could have polluted the samples during the mechanical enrichment process. In the next step the components sulfur and arsenic shall be removed by oxidation and sublimation in a gas chemistry procedure, which would prevent contamination by external chemicals. The oxidation should be performed in a quartz apparatus to prevent contaminations. With neutron- activated Lorandite volatilisation yields of ^{76}As were measured to be about 99%. After dissolving the residue in purest hydrochloric acid and oxidation by bromine Tl^{3+} can be extracted in di-isobutyl-ether with high yield. Chlorine is a better oxidising agent, but to prevent formation of Pb^{4+} Br_2 is better suited. Di-ethyl-ether could be used as extractant, too. The disadvantage is a relatively high danger of peroxides which are no problem when using di-isobutyl-ether. In the concentration region between 6n HCl and 8n HCl after 4 extractions the aqueous phase contained $< 10^{-6}$ of the original activity. In the next step traces of Tl^{3+} can be adsorbed on ammonium phosphomolybdate, $(\text{NH}_4)_3[\text{P}(\text{Mo}_3\text{O}_{10})_4] \times 6 \text{H}_2\text{O}$, or prussian blue, $\text{Fe}_4[\text{Fe}(\text{CN})_6]_3$ after reduction from Tl^{3+} to Tl^{1+} with SO_2 . The Tl- solutions succed through thin layers of this scavenging precipitates contained 7×10^{-5} of the original Tl in the case of ammonium phosphomolybdate, and $< 2 \times 10^{-5}$ for prussian blue.

A final purification can be made by a anion exchange procedure which separates Tl^{3+} from Pb^{2+} better than 5 orders of magnitude. With a 5cmx3mm column of standard anion exchanger (Dowex 1-X8 minus 400mesh) the Tl content of the eluate with 0.1n HCl was below the detection limits of 10^{-6} . Special precautions must concern the Pb- and Tl- content of the used chemicals which should be kept below pg/g, if possible. The final separations must be done in dust- free hoods in quartz vessels.

Before the precious Lorandite is worked up one should perform the separation with realgar (As_2S_3) or oripiment (As_2S_2) from the same geological deposit to verify that lead in these samples free from thallium does not contain significant traces of ^{205}Pb .

References

- /1/ M. S. Freedman, C. M. Stevens, E. P. Horwitz, L. H. Fuchs, J. S. Lerner, L. S. Goodman, W. J. Childs, J. Hessler, Science 193 (1976) 1117
- /2/ M. K. Pavićević, Nucl. Instr. and Meth. A271 (1988) 287
- /3/ W. Henning, D. Schüll, Nucl. Instr. and Meth. A271 (1988) 324
- /4/ G. Korschinek, J. Sellmair, A. Urban, M. Müller, Nucl. Instr. and Meth. A271 (1988) 328
- /5/ M. Krčmar, S. Kaučić, A. Ljubičić, T. Tustonić, I. Žilimen, R. Ilić, T. Šutej, B. Logan, Symposium on Solar Neutrino Detection, Dubrovnik 9.-12.10.90

Trace Analysis of Technetium in a Laser Ion Source

F. Ames, T. Brumm, K. Jäger, H.-J. Kluge, B.M. Suri*, A. Venugopalan*

Institut für Physik, Universität Mainz, D-6500 Mainz

H. Rimke, N. Trautmann, Institut für Kernchemie, Universität Mainz, D-6500 Mainz

R. Kirchner, GSI, D-6100 Darmstadt

Isotopic analysis of small amounts of technetium chemically separated from molybdenum ore can throw light on the integral ^8B solar-neutrino flux over the past several million years. In the case of the Henderson Rock Mine (Colorado) such an experiment involves the detection of about 10^8 atoms of $^{97,98}\text{Tc}$ out of 5000 t of ore produced from molybdenum by an inverse β -decay induced by solar neutrinos. In addition, such a sample will contain about 10^{11} atoms of ^{99}Tc from spontaneous fission of uranium and about 10^{15} atoms of molybdenum even after chemical separation [1][2]. As a consequence, high sensitivity and high elemental and isotopic selectivity are required. Since the uranium content of the ore is known, only the relative abundance of $^{97,98}\text{Tc}$ in respect to ^{99}Tc has to be measured. This can be done by resonance ionization mass spectroscopy (RIMS).

The sample under investigation is evaporated and the atoms are excited resonantly in several steps to a highly excited atomic state by the absorption of laser light. Finally, they are ionized by the absorption of an additional photon or by applying an electrical field. These photoions can be detected via mass spectrometry.

In order to improve the efficiency compared to conventional RIMS experiments with a thermal atomic beam crossed by perpendicular laser beams, a hot cavity is used with a small hole to inject the laser beams and to extract the photoions. Thus, the atoms are confined inside the cavity and have the chance to cross the interaction region with the laser beams several times. Using high-repetition rate lasers like copper vapor laser pumped dye lasers ($\nu_{rep} = 6.5$ kHz) an efficiency of several 10% can be reached.

We have built up such a laser ion source for trace analysis of Tc at Mainz. A temperature of more than 2300 K is required for the evaporation of Tc. This can be obtained by use of a tungsten or graphite cavity heated by electron bombardment, a design developed at GSI as an ion source at the on-line mass separator [3]. Such a laser ion source with a hole diameter of 2.7 mm, an inner diameter and a length of 1 cm can reach theoretically an efficiency of 17 % for the photo ionization of technetium at a temperature $T = 2400$ K [4]. The extracted ions are focused to the entrance slit of a Mattauch-Herzog mass spectrometer.

Technetium is ionized by a three-step, three-colour resonant excitation to an autoionizing state ($\lambda_1 = 313.12$ nm, $\lambda_2 = 821.13$ nm, $\lambda_3 = 670.74$ nm). The technetium was deposited electrolytically on a small rhenium filament [5] and introduced into the cavity. Until now samples containing $5 \cdot 10^8$ to 10^{12} atoms ^{99}Tc were used. A total efficiency of $4 \cdot 10^{-4}$ for the whole apparatus was obtained. This value includes the transmission and detection efficiency of $3 \cdot 10^{-3}$ of the mass spectrometer. Thus the efficiency of the source is 14 %, very close to the theoretical value. The efficiency was shown to be sufficient for the solar-neutrino experiment, but there is still an interference of thermally ionized molybdenum occurring as an impurity in the cavity material. This background can be reduced using the pulsed structure of the photoion beam.

Figure 1 shows a typical result of a measurement. In this case, $1.5 \cdot 10^9$ atoms of ^{99}Tc were loaded into a graphite cavity and heated up to nearly 2300 K. The upper part of the figure shows a mass spectrum ($A = 92$ to $A = 100$) with the laser beams blocked. Only thermally ionized molybdenum can be seen. If the lasers are on and set on resonance for ^{99}Tc (middle of figure 1) the molybdenum signal remains constant but an additional peak appears at mass $A = 99$. The lower part shows the same signal but with a coinci-

dence gate ($4.5 \mu\text{s}$) for the photoions. The ratio of photoion signal to thermal ion background is increased by nearly a factor of 10. The background can be reduced further by using purer materials for construction of the cavity or materials with lower work function for reduced thermal ionization efficiency.

Supported by the Deutsche Forschungsgemeinschaft

* Permanent address : Bhabha Atomic Research Centre, Bombay-400085, India

- [1] G. Cowan, W. Haxton, Science 216:51 (1982)
- [2] N. Nogar, R. Sander, S. Downey, Proc. Soc. Photo-Opt instr. Eng. 380:291 (1983)
- [3] R. Kirchner et al., Nucl. Instr. Meth. 186:295 (1981)
- [4] F. Ames, T. Brumm, K. Jäger, H.-J. Kluge, B. M. Suri, H. Rimke, N. Trautmann, R. Kirchner, Appl. Phys. B 51:200 (1990)
- [5] P. Sattelberger, M. Mang, G. Herrmann, J. Riegel, H. Rimke, N. Trautmann, F. Ames, H.-J. Kluge, Radiochimica Acta 48:165, (1989)

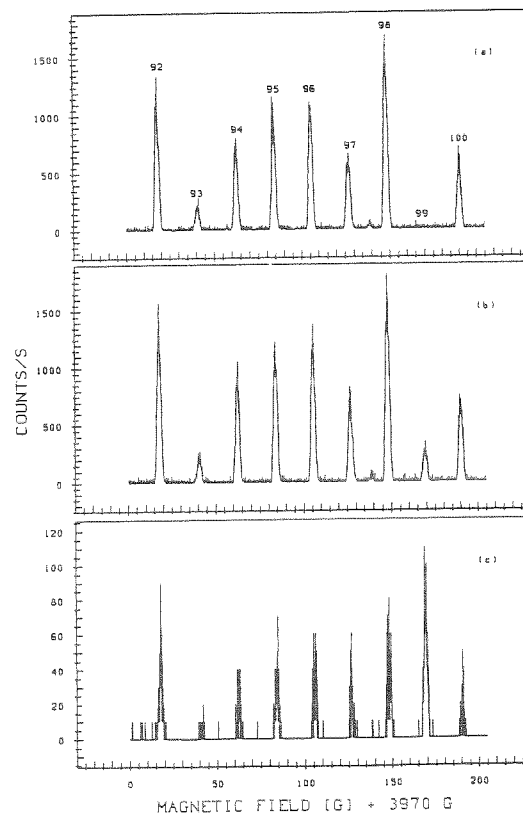


Fig. 1 Part of the mass spectrum ($A = 92$ to $A = 100$) from a graphite cavity containing $1.5 \cdot 10^9$ atoms of ^{99}Tc . a) Laser beams shut off, b) laser beams on and in resonance for ionization of ^{99}Tc , c) same as b) but gated detection.

Chemical Properties of Element 105 in Aqueous Solution: Further Studies of the Halide Complex Extraction into Triisooctyl Amine ^B

H.P. Zimmermann, J.V. Kratz, M.K. Gober, Institut für Kernchemie, Universität Mainz

M. Schädel, W. Brüchle, E.Schimpf, GSI, Darmstadt

H. Gäggeler, D. Jost, J. Kovacs, U.W. Scherer, A.Weber, PSI, Villigen, Switzerland

K.E. Gregorich, A. Türler, B. Kadkhodayan, K.R. Czerwinski, N.J. Hannink, D.M. Lee, M.J. Nurmi,
D.C. Hoffman, Lawrence Berkeley Laboratory, Berkeley, California

Previously, we have performed anion exchange separations of 34-s $^{262}_{105}\text{Ha}$ from HCl and mixed HCl/HF solutions [1] using reversed-phase micro-chromatographic columns incorporating triisooctyl amine (TIOA) on an inert support in the computer-controlled liquid chromatography apparatus, ARCA II [2]. $^{262}_{105}\text{Ha}$ was shown to be adsorbed on the column from either 12 M HCl/0.02 M HF or 10 M HCl solutions like its homologs Nb and Ta, and like Pa. In elutions with 4 M HCl/0.02 M HF (Pa-Nb fraction), and with 6 M HNO_3 /0.015 M HF (Ta fraction), the $^{262}_{105}\text{Ha}$ activity was found in the Pa-Nb fraction showing that the anionic halide complexes are different from those of Ta, and are more like those of Nb and Pa. In separate elutions with 10 M HCl/0.025 M HF (Pa fraction), and 6 M HNO_3 /0.015 M HF (stripping of Nb), the $^{262}_{105}\text{Ha}$ was found to be equally divided between the Pa and Nb fractions. The non-tantalum like halide complexation of element 105 is indicative of the formation of oxohalide or hydroxohalide complexes, like $[\text{NbOCl}_4]^-$ and $[\text{PaOCl}_4]^-$ or $[\text{Pa}(\text{OH})_2\text{Cl}_4]^-$, in contrast to the pure halide complexes of Ta, like $[\text{TaCl}_6]^-$.

We have extended the elution studies of the group-VB elements from TIOA columns in ARCA II to 0.5 M HCl/0.01 M HF as the effluent. 34-s $^{262}_{105}\text{Ha}$ from the ^{249}Bk ($^{18}\text{O}, 5\text{n}$) reaction at 99 MeV beam energy was produced at the LBL 88-inch cyclotron and transported on-line by a He/KCl jet to the chemistry apparatus where it was collected on a polyethylene frit. After a collection time of 60 s the frit was washed with 12 M HCl/0.01 M HF which dissolved the activities, and assured chloride complexing of the group-VB elements. This solution passed through one of the TIOA-Voltaef mini columns ($1.6 \times 23 \text{ mm}$) where the homologs Nb and Ta, as well as the pseudo homolog Pa, were extracted, while the group-IVB elements and the actinides were eluted from the column.

In 345 elutions with 0.5 M HCl/0.01 M HF (Pa fraction) and with 4 M HCl/0.02 M HF (Nb fraction), the $^{262}_{105}\text{Ha}$ activity was found in the Pa fraction. Ta is not eluted from TIOA under these conditions. In order to determine the elution position of element 105 more accurately, we have cut the Pa fraction after 4.5 s into an "early Pa fraction", and a "late Pa fraction" (elution with 0.5 M HCl/0.01 M HF for another 7.0 s). In the "early Pa fraction" containing about 25 % of the Pa tracer activity, we observed 8 $^{262}_{105}\text{Ha}$ decays (38 %), while in the "late Pa fraction", containing about 75 % of the Pa tracer activity we observed 13 $^{262}_{105}\text{Ha}$ decays (62 %). These are the results of 228 experiments. Within the error limits, the hahnium distribution is not significantly different from the Pa distribution, even

though one might recognize that hahnium elutes slightly earlier than Pa.

The elution positions can be transformed into distribution coefficients; the latter are expressed as fraction contained in the organic phase in Fig.1, together with the respective data for Zr, Hf, Nb, Ta, and Pa [1]. The results from our previous work at 10 M HCl and 4 M HCl, and the results of the present work at 0.5 M HCl indicate that the distribution coefficients for hahnium follow in detail the ups and downs in the coefficients for Nb and Pa, and that the extraction behavior of hahnium is very different from that of Ta over a wide range of HCl concentrations.

In summary, the close analogy [1] of the chemical behavior of hahnium to protactinium, and to niobium, is confirmed also for low HCl concentrations. This strengthens our case for the formation of oxo- or hydroxohalide complexes by hahnium.

[1] J.V. Kratz et al., *Radiochim. Acta*, **48**, 121 (1989)

[2] M. Schädel et al., *Radiochim. Acta*, **48**, 171 (1989)

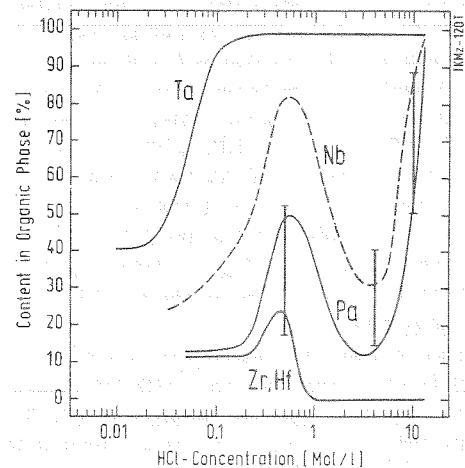


Fig.1 Fraction extracted into TIOA vs HCl concentration
The vertical bars represent the behavior of element 105.

Chemical Properties of Element 105 in Aqueous Solutions: Diisobutylcarbinol Extractions ^G

M.K. Gober¹, J.V. Kratz¹, H.P. Zimmermann¹, W. Bröchle², M. Schädel², E. Schimpf², H. Gäggeler³,
D. Jost³, J. Kovacs³, U.W. Scherer³, A. Weber³, K.E. Gregorich⁴, A. Türler⁴, B. Kadkhodayan⁴,
K.R. Czerwinski⁴, R.A. Henderson⁴, D.M. Lee⁴, M.J. Nurmi⁴, D.C. Hoffman⁴,

¹Institut für Kernchemie der Universität Mainz, ²Gesellschaft für Schwerionenforschung, Darmstadt

³Paul Scherrer-Institut, CH-5303 Würenlingen, ⁴Lawrence Berkeley Laboratory, Berkeley, California

The secondary alcohol diisobutylcarbinol (DIBC) is known to be a very specific extractant for protactinium halide complexes [1]. A standard separation of Pa involves the extraction into DIBC from 9 - 12M HCl and its back extraction in 12M HCl/0.25M HF or dilute HCl solutions [1]. Since we have found evidence for a close similarity in the halide complexation and extraction into triisooctylamine between protactinium, niobium, and element 105 [2], it was attractive to test the potential of DIBC for extractions of element 105.

We have determined the distribution coefficients of Zr, Nb and Pa for DIBC extractions from HCl, HBr and HF solutions in a series of batch experiments. Some results are shown in Fig. 1. It was the aim of these experiments to find conditions under which the prototypes for element 105, Pa and Nb, are both extracted quantitatively into DIBC. Fig. 1 shows that the HCl/DIBC system does not meet this requirement. The insufficient extraction of Nb in this system even at high HCl concentrations is likely to be due to the formation of polynegative anions such as $[\text{NbOCl}_6]^{2-}$. The dielectric constant of DIBC is not large enough to accommodate polynegative species. In conc. HBr, the required simultaneous extraction of Nb and Pa into DIBC is fulfilled better. Therefore, we have adopted the HBr/DIBC system to HPLC separations, and have tested both the initial extraction of Pa and Nb, as well as possibilities for their separate elution. Teflon columns (2×20 mm) filled with DIBC-coated Voltalef powder (weight ratio 1:3) were used. The best conditions were as follows: After the extraction of Nb and Pa into DIBC from conc. HBr, a Nb fraction was eluted from the column in 6M HCl/0.0002M HF, followed by the stripping of Pa from the column in 0.5M HCl. The separation was subsequently implemented at the ARCA II apparatus [3]. The separation is depicted in Fig. 2. Unfortunately, losses of about 15% of Nb in the feeding of the activities onto the columns were inevitable.

The same separations were performed with $34\text{-s }^{262}_{106}\text{Ha}$ produced at the LBL 88-inch Cyclotron in the $^{249}\text{Bk}(^{18}\text{O},5n)$ reaction. Low extraction yields were observed throughout: In a first series of 99 experiments no α - and 4 SF decays attributable to ^{262}Ha were recorded in the Nb fraction. In order to exclude that the elution conditions chosen were inadequate for hahnium, we checked the extraction yield of ^{262}Ha into the DIBC phase by feeding the activity to the column, and by stripping the DIBC (along with the extracted activities) from the columns by dissolving it in acetone. The acetone strip fraction was evaporated to dryness, and assay of the sample for α - and SF decay started 48s after the end of the collection cycle. In 240 experiments 6 α - and 7 SF decays were recorded. Comparison of the "apparent" cross section resulting from these decay rates, 4.4 nb, with the known production cross section at 99MeV beam energy, 8.3 ± 2.4 nb, gives an extraction yield of roughly 50%. Subsequently, we have continued elutions of Nb fractions in 6M HCl/0.0002M HF from the columns and

have detected another 6 α - and 3 SF events, compatible within the uncertainties with the reduced extraction yield mentioned above. These results show, that the tendency to form polynegative complex species in conc. HBr increases in the sequence $\text{Pa} < \text{Nb} < \text{Ha}$. The experiments do not allow to decide whether this reflects an increase in the equilibrium constant for $[\text{MeOBr}_4]^- + \text{Br}^- \rightleftharpoons [\text{MeOBr}_5]^{2-}$, or whether the kinetics for the back reaction of $[\text{MeOBr}_5]^{2-}$ into the extractable species $[\text{MeOBr}_4]^-$ is slower for Ha than for Nb and Pa.

References:

- [1] N. Trautmann et al., *Radiochim. Acta* 11, 168 (1969)
- [2] J. V. Kratz et al., *Radiochim. Acta* 48, 121 (1989)
- [3] M. Schädel et al., *Radiochim. Acta* 48, 171 (1989)

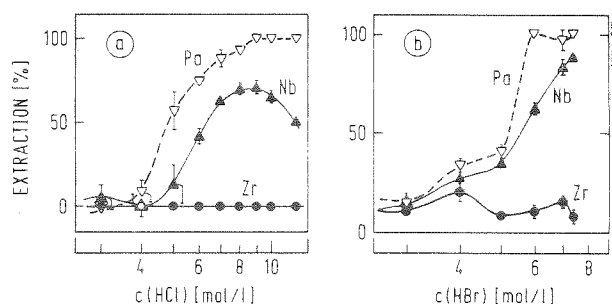


Fig. 1: Percentage extraction of Zr, Nb, and Pa into DIBC from (a) HCl solutions and (b) HBr solutions.

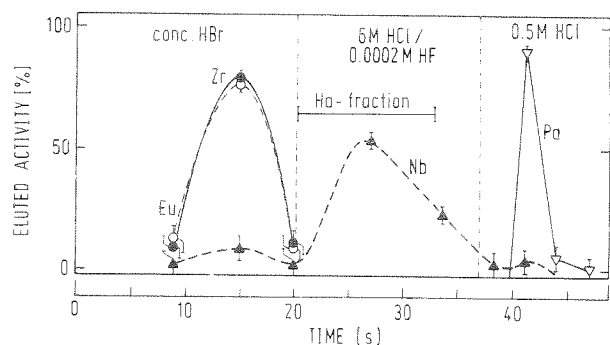


Fig. 2: Separation of Eu, Zr, Nb, and Pa on a 1.6×23 mm DIBC - Voltalef column in ARCA II. The flow rate for feeding the activities onto the column in conc HBr was 0.5 ml/min. The elutions occurred at 1 ml/min.

Fast α -HIB Separations of Element 105^{G,B}

H.P. Zimmermann, J.V. Kratz, M.K. Guber, Institut für Kernchemie, Universität Mainz
M. Schädel, W. Brüchle, E. Schimpf, GSI, Darmstadt

H. Gäggeler, D. Jost, J. Kovacs, U.W. Scherer, A. Weber, PSI, Villigen, Switzerland

K.E. Gregorich, A. Türler, B. Kadhodayan, K.R. Czerwinski, N.J. Hannink, D.M. Lee, M.J. Nurmi,
D.C. Hoffman, Lawrence Berkeley Laboratory, Berkeley, California

In 1990, we have investigated further the chemical properties [1] of element 105 in aqueous solution. A newly developed separation procedure is based on the following consideration: The complexing strength of α -hydroxy-iso-butyric acid (α -HIB) increases with the ionic charge of the metal ion. Thus, if element 105 forms pentavalent metal ions in aqueous solutions, it will be more strongly complexed than tetravalent or trivalent metal ions. By feeding an α -HIB solution of appropriate concentration and pH to a cation exchange column, one expects pentavalent metal ions (element 105) to be immediately eluted from the column, while tetravalent ions (element 104) are retained on the column. This is even more the case for the trivalent actinides.

We have tested this chemical procedure in manually performed HPLC separations [2] using tracer activities of ^{96}Zr , ^{96}Nb and ^{233}Pa produced at the Mainz TRIGA reactor. Subsequently, the procedure was implemented at the Automatic Rapid Chemistry Apparatus, ARCA II [3]. First on-line experiments were performed with $^{168-170}\text{Ta}$ produced at the UNILAC accelerator [2], and with short lived Nb isotopes produced at the TRIGA reactor. The reaction products were transported from the target to a collection frit by a He/KCl gas jet system. After 1 min, the products were dissolved in unbuffered 0.05 M α -HIB and eluted from 1.6×8 mm chromatographic columns containing the strongly acidic cation exchange resin Aminex A6 (particle size $17.5 \pm 2 \mu\text{m}$). An elution curve for Nb is shown in Fig. 1. In less than 4 s more than 90 % of the activity elutes from the column. The small effluent volume ($50 \mu\text{l}$) is quickly evaporated to dryness using intense IR light and a stream of hot He gas.

The method was applied to 34-s $^{262}_{106}\text{Ha}$ produced in the ^{249}Bk ($^{18}\text{O}, 5n$) reaction at 99 MeV bombarding energy. The resulting α -particle spectrum is shown elsewhere in this report [4]. Apart from a contamination by ^{249}Cf sputtered from the target (this material is not dissolved in the weakly acidic α -HIB solution and is washed mechanically through the column), and by a small Bi and Po activity produced by transfer reactions on a Pb impurity in the target, the spectrum is extremely clean and compatible with the complex spectra of $^{262}_{106}\text{Ha}$ and its daughter ^{258}Lr . These assignments are corroborated by 9 correlated pairs of mother-daughter decays with the correct half-life of $4.2 \pm_{1.1}^{1.5}$ s for the correlated daughters. The results provide an independent proof of the 5+ oxidation state of element 105 in aqueous solution.

Also, the high decontamination from interfering actinides makes this separation procedure a very powerful tool for the isolation of hahnium isotopes for spectroscopic study. As a first result, we report on the discovery of the new isotope $^{263}_{106}\text{Ha}$ produced in the ^{249}Bk ($^{18}\text{O}, 4n$) reaction [4].

The small volume of the separated Ha-fractions also opens the possibility to elute directly onto the surface of a 2700mm² Passivated Implanted Planar Silicon (PIPS, Canberra) detector for the measurement of α - and SF-decays. In order to obtain a

reasonable energy-resolution, the thickness of the liquid should not exceed some ten μm . The variable thickness is defined by a titanium surface opposing the surface of the PIPS detector, the thickness being measured by inductive gauge heads (TESA). The resulting volume is sealed by a silicon rubber ring pressed onto the detector surface at its outer edge. The titanium surface contains a central bore hole through which the liquid is introduced and twelve holes at its outer edge serving as outlets. The thickness was adjusted to $23 \mu\text{m}$ resulting in a calculated volume of $56 \mu\text{l}$ which is sufficient to accommodate the α -HIB eluate. In tests with $^{212}\text{Bi}/\text{Po}$ solutions an α -energy resolution of about 500 keV was obtained.

In the 105-experiments, the effluent was pumped into the chamber and assayed for α - and SF-events for one minute. In 392 α -HIB separations, 11 α - and 9 SF-events were observed. Based on the known cross section, and by assuming a counting efficiency of 50%, one would have expected to see eight times this number of events. The reduced efficiency is likely to be connected to the optically apparent fact that the detector surface was not planar, making the effective volume of the counting cell much smaller than calculated. A new detector construction with improved surface planarity is being developed.

[1] J.V. Kratz et al., *Radiochim. Acta* 48, 121 (1989)

[2] H.P. Zimmermann et al.,
GSI Scientific Report 1989, p.239

[3] M. Schädel et al., *Radiochim. Acta* 48, 171 (1989)

[4] J.V. Kratz et al., this report

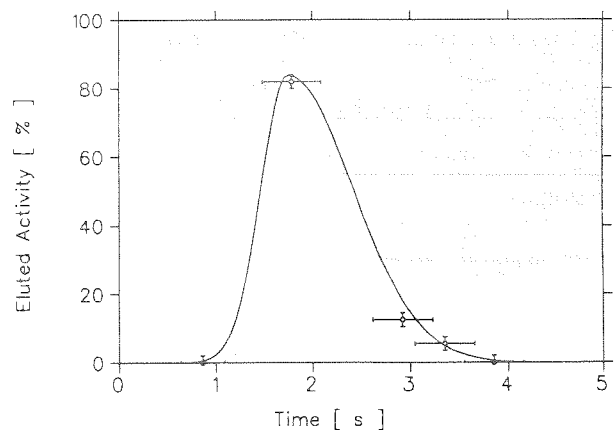


Fig.1 Elution curve for Nb in 0.05 M α -HIB from a 1.6×8 mm cation exchange column in ARCA II at a flow rate of 1 ml/min.

Gaschemistry Experiments with Bromides of Niobium, Tantalum and Element 105 ^{G, B}

H.W. Gäggeler, D.T. Jost, J. Kovacs, U.W. Scherer, A. Weber, D. Vermeulen
 Paul Scherrer Institut, Villigen, Switzerland
 J.V. Kratz, M.K. Gober, H.P. Zimmermann
 Institut für Kernchemie, Universität Mainz
 M. Schädel, W. Brüchle
 GSI, Darmstadt
 I. Zvara

Joint Institute for Nuclear Research, Dubna, USSR
 A. Türler, K.E. Gregorich, R.A. Henderson, K.R. Czerwinski, B. Kadkhodayan,
 D.M. Lee, M. Nurmia, D.C. Hoffman
 Lawrence Berkeley Laboratory, Berkeley, USA

Recently, considerable interest has been drawn to the study of the chemistry of the transactinide elements (atomic number > 103) from both experimental and theoretical chemists. Relativistic effects may affect the configuration of valence electrons to such an extent that the chemical properties of these elements may not longer be extrapolated from their lighter homologs in the periodic table. Recent extensive theoretical calculations^{1,2,3} have now provided chemists with predictions on how the relativistic rearrangements of valence electrons affect the chemical properties of the heaviest elements and in which compounds these effects should become noticeable.

We have developed an on-line gaschemistry apparatus (OLGA)⁴ which allows to continuously separate volatile atoms or molecules of different volatility.

An improved version, OLGA II, is shown in Fig. 1. Products transported by a He/KCl Gas-jet system are continuously injected in a quartz column. Behind the isothermal column the ejected molecules are reattached onto new KCl particles and transported through a capillary to a counting station. This device is a rebuilt magnetic tape station. Products are collected on the surface of a tape and - from time to time - transported through 6 counting chambers equipped with PIPS (passivated ion-implanted planar silicon) detectors. This allows to detect α - and β -activities in a 2π geometry.

OLGA II was used to investigate the volatility of the group VB pentabromide molecules NbBr₅, TaBr₅ and HaBr₅ by isothermal gaschromatography in empty quartz columns. Short-lived isotopes ($T_{1/2} \leq 1$ min) of those elements were produced at the reactor SAPHIR (Nb⁵) and at the 88-inch cyclotron in Berkeley (Ta, Ha) in the fusion reactions of 120 MeV ²⁰Ne + ¹⁴⁷Sm and 100 MeV ¹⁸O + ²⁴⁹Bk, respectively. After collecting the KCl particles on a quartz wool plug the bromide molecules of Nb, Ta and Ha were formed by adding 100 ml/min HBr gas (Nb, Ha) or 100 ml/min HBr gas saturated with BBr₃ vapour (Ta). As chemical signal the activity behind the quartz chromatography column was measured as a function of the temperature of the tube. The temperature at the quartz wool plug was kept constant at about 900 °C.

Fig. 2 depicts the chemical yields of bromide molecules formed with ⁹⁹Nb ($T_{1/2} = 15$ s), ¹⁶⁶Ta ($T_{1/2} = 35$ s) and ²⁶²Ha ($T_{1/2} = 35$ s), respectively. ⁹⁹Nb and ¹⁶⁶Ta were detected via their γ -lines and ²⁶²Ha by its sf-decay (see Fig. 3). From Fig. 2 we read that the volatilities of Nb and Ta bromide are very similar. Ha-bromide, however, has a significantly lower volatility relative to those of Nb and Ta. Adding BBr₃ vapour to HBr did not change the yield curve of hahnium.

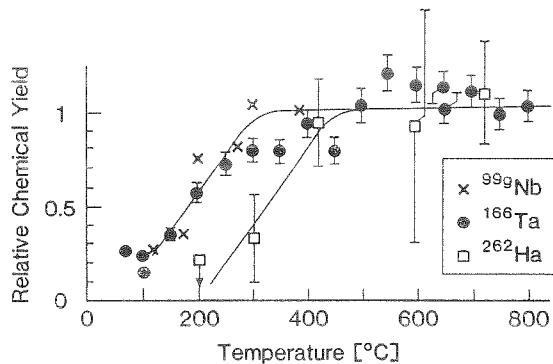


Fig. 2: Relative chemical yields (maximum yield = 1) of Nb-5, Ta- and Ha-bromide molecules behind an empty, isothermal quartz chromatography column. As reactive gases HBr (Nb, Ha) and HBr/BBr₃ (Ta) were used.

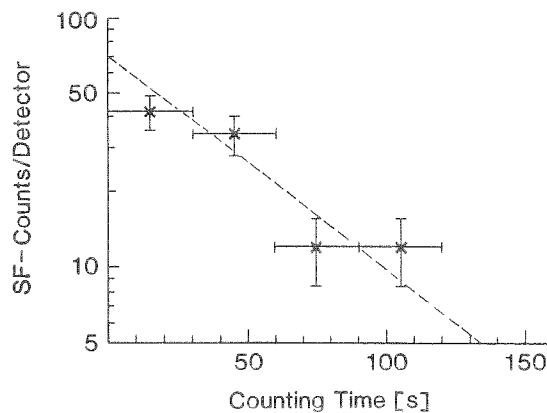


Fig. 3: Spontaneous-fission activity measured behind the chromatography column with HBr as reactive gas. Based on the half-life this activity is attributed to ²⁶²Ha.

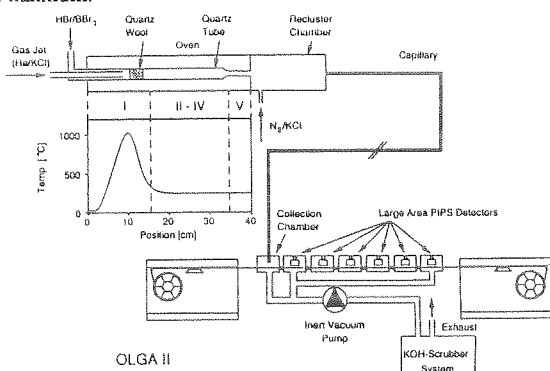


Fig. 1: Schematic of OLGA II, a system for continuous separation and detection of volatile species.

- 1 V.A. Glebov et al., Radiochim. Acta **46**, 117 (1989).
- 2 B.L. Zhuikov et al., Radioanal. Nucl. Chem., **143**, 103 (1990).
- 3 E. Johnson et al., J. Chem. Phys., in press.
- 4 W. Brüchle et al., J. Less Comm. Metals, **122** (1986) 425.
- 5 Ya Nai-Qi et al., Radiochim. Acta **47**, 1 (1989).

On the Volatility of Protactinium Bromide ^{G, B}

D.T. Jost, H.W. Gäggeler, A. Weber, A. Kovacs, U. Scherrer, M. Schwikowski
Paul Scherrer Institut, Villigen, Switzerland

W. Bröchle, M. Schädel, G. Schimpf
GSI, Darmstadt

J.V. Kratz, H.P. Zimmermann, M.K. Gober
Institut für Kernchemie, Universität Mainz

B. Eichler
Zentralinstitut für Kernforschung, Dresden

In the course of experiments to investigate the chemical properties of element 105, hahnium, it was found that the volatility of HaBr_5 is significantly lower than those of the group VB homologs TaBr_5 and NbBr_5 . It was argued that possibly Ha behaves more like the pseudo-group V element Pa. However, detailed knowledge on the volatility of PaBr_5 is lacking.

We have studied the gaschromatographic behaviour of protactinium bromide in quartz columns in a similar way as for the group VB elements Nb, Ta and Ha¹. The short-lived isotope ^{226}Pa ($T_{1/2} = 2.6$ min) was used as tracer, produced at Injector I of PSI in the reaction $58 \text{ MeV } p$ on a $100 \mu\text{g}/\text{cm}^2$ ^{232}Th target. For continuous transportation of ^{226}Pa a He/KCl gas-jet system was used. Products were transported along a 700 m polyethylene capillary to the on-line gaschemistry apparatus OLGA. In order to maintain a flow rate of about 1 l/min a pressure in the target chamber of about 4,5 bar was needed. The transportation yield and time were found to be about 10%, and 1 min, respectively². 100 ml/min pure HBr or HBr saturated with BBr_3 vapour was added to the position of the quartz wool plug in the chromatography column (see Fig. 1 in ¹). Behind the column, molecules were reattached onto new KCl particles and transported to the tape counting system. ^{226}Pa was measured with 450 mm² PIPS (passivated ion-implanted planar silicon) detectors via its α -decay chain. For the first time the data were stored in an event-by-event mode with the PSI-TANDEM³ system and analyzed with the CERN-PAW⁴ software. This allowed to identify also α - α -correlations. Figures 1a and b show measured time correlations between α -events from the 6.47 MeV decay line of ^{226}Pa and those of the 4,2 s daughter 7.01 MeV ^{222}Ac and from the 700 μs daughter 7.87 MeV ^{218}Fr , respectively.

Fig. 2 depicts the measured chemical yields as a function of the oven temperature using different reactive gases. Only with HBr/BBr_3 reasonable maximum yields of about 40 % were observed above 300 °C. With pure HBr and HCl the formation of the penta-halides seems to be hindered. The experiments have to be repeated in order to carefully determine the slope of the yield curve for $T \leq 300$ °C with HBr/BBr_3 and to try also strongly chlorinating substances such as SOCl_2 .

Acknowledgement:

We highly appreciate the ^{232}Th targets made by H. Folger.

¹ H. Gäggeler et al., this annual report.

² A. Weber, Internal Report Paul Scherrer Institut, PSI-TM-32-90-06 (1990).

³ F.W. Schlepütz, IEEE Trans. Nucl. Sci. **36** (5), 1630 (1989).

⁴ R. Brun et al., CERN Program Library Entry Q121, Geneva (1989).

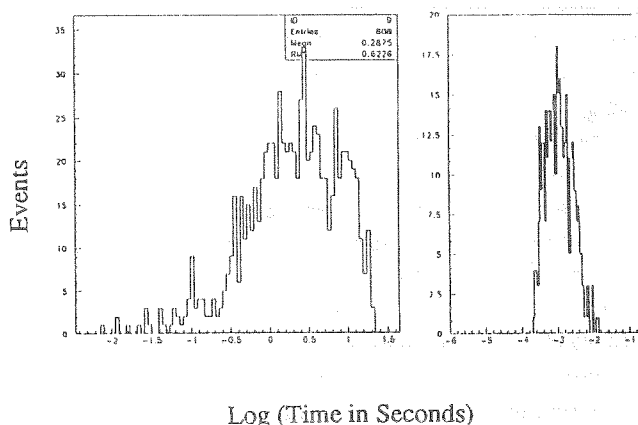


Figure 1 a (left): Time correlations between α -events from ^{226}Pa and ^{222}Ac .
Figure 1 b (right): Between ^{222}Ac and ^{218}Fr .

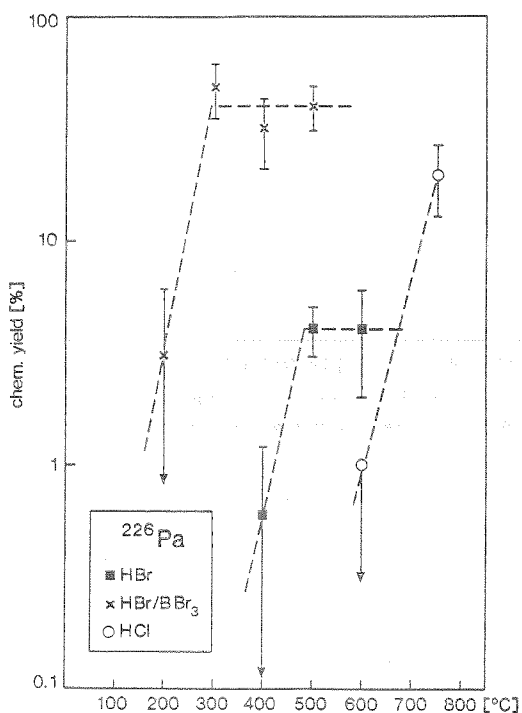


Figure 2: Chemical yields for protactinium halides behind an isothermal empty quartz column, using different reactive gases.

V. Pershina, W.-D. Sepp, B. Fricke
Physics Department, University of Kassel

Solution chemistry experiments on the complex formation of the group V elements by exchange solvent extraction^{1,2} have shown that 105 element compounds behave differently from what could be expected as a straightforward extrapolation of the properties within the group. The non-tantalum like halide complexation of Ha was indicative of the formation of oxohalide complexes like $[\text{NbOCl}_4]^-$ and $[\text{PaOCl}_4]^-$ for intermediate HCl concentrations in contrast to the pure halide complexes $[\text{TaCl}_6]^-$.

The different complexing ability of the group V elements is connected with the electronic structure of the central ion (metal) and a character of its interaction with ligands. To understand the nature of the chemical bonding in those compounds the electronic structure of the following species have been calculated: $[\text{MCl}_6]^-$ and $[\text{MOCl}_4]^-$, where $\text{M}=\text{Nb, Ta, Pa}$ and Ha . Oxochloride complexes were supposed to have C_{4v} symmetry and chloride ones - O_h . Variations in the bond distances and angles have been taken into consideration.

The calculations have been done using relativistic Dirac-Slater code³.

As a result of calculations it was shown that Ha forms double $\text{Ha}=\text{O}$ bond as in case of $[\text{NbOCl}_4]^-$ and $[\text{NbOCl}_5]^-$. Variations in the metal-ligand distances do not influence much the data on electronic density distribution. Results of the analysis of the charge density distribution is shown in Table 1.

Table 1
Mulliken analysis data for $[\text{MOCl}_4]^-$

Parameter	$[\text{NbOCl}_4]^-$	$[\text{TaOCl}_4]^-$	$[\text{PaOCl}_4]^-$	$[\text{HaOCl}_4]^-$
$n(k)$	39.066	70.847	89.188	102.977
$N(k)$	40.163	72.133	90.132	104.282
$n(k,l)$	2.187	2.618	2.189	2.729
Q	0.836	0.867	0.868	0.718

where $n(k)$ - nett atomic population; $N(k)$ - gross atomic population; $n(n,k)$ - overlap population, Q - effective atomic charge.

As in case of MCl_5 and MBr_5 the chemical bond strength increases from Nb compound to Ta one in its two constituents: the ionic and covalent, while in going from Ta complex to Ha one the increase in covalent contribution is partially compensated by decrease in ionic part.

Results of the $[\text{MCl}_6]^-$ complexes calculations have revealed an interesting fact that in opposite to the oxochloride series in the row $[\text{NbCl}_6]^-$, $[\text{TaCl}_6]^-$, $[\text{PaCl}_6]^-$ the overlap metal-ligand does not increase from Ta to Ha but for some interatomic distances even decreases (2.470, 2.971 and 2.948 correspondingly). Obviously the tendency of Ta to form the six-coordinated compounds is more pronounced than in case of hanium while the tendency of Ha to form the double bond with oxygen is the strongest in the series (the metal-oxygen overlap

populations for complexes of Nb, Ta, Pa and Ha are 0.65, 0.79, 0.52 and 0.86 respectively).

Stability in aqueous solutions is determined also by hydration enthalpy, which according to the Born-Bjerrum theory of ionic solvation is a functional dependence of z^2/r , where r is an ill-defined ionic radius, or in our case the size of the anion. Taking into account the big ionic radius of Ha^{5+} (0.0736 nm according to multiconfigurational Dirac-Fock calculations⁴) the ΔY_{hyd}^0 should be the smallest in case of big complexes of the 105 element.

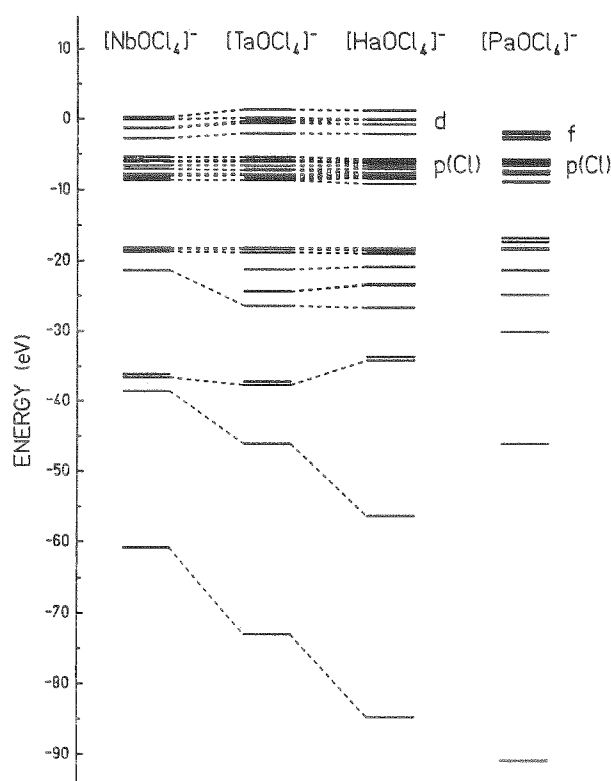


Fig.1: Energy eigenvalues of the outer electrons for $[\text{MOCl}_4]^-$

References

1. Kratz J.V., Zimmermann H.P., Scherer U.W. et al., Radiochim. Acta 48, 121-133 (1998).
2. Schädel M. "Radiochemical studies of the transactinide elements", GSI-89-72 Preprint, October 1989
3. Rosen A. et al., J.Chem.Phys., 62, 3039 (1975)
4. Fricke B. and Johnson E., in press.

V. Pershina, W.-D. Sepp, B. Fricke
Physics Department, University of Kassel

It is well known that close to the end of the periodic Table relativistic effects start to play an important role influencing atomic characteristics such as binding energies, atomic (ionic) radii, etc. This in its turn effects physics and chemistry of the heavy and superheavy elements leading to altering their chemical behavior. Thus peculiarities of the superheavy elements behavior compared to their analogs in the gas-phase experiments on the volatility of the halides of 104 and 105-elements^{1,2} have given a strong impact to investigations of their electronic structure.

Relativistic self-consistent Dirac-Slater calculations³ of the halides of the group V elements have been done to understand the reasons for the differences in their physico-chemical properties. The objects of interest were chlorides and bromides: NbCl₅, TaCl₅, PaCl₅, HaCl₅ (and VCl₅ for comparison) and NbBr₅, TaBr₅, PaBr₅, HaBr₅. Experimental geometrical structure (D_{3h}) and interatomic distances have been taken for the compounds of Nb and Ta. The Ha halides were supposed to have the same geometry with Ha-ligand distance being estimated from Dirac-Fock multiconfigurational calculations. Calculations of Pa halides however have shown that PaCl₅ and PaBr₅ molecules are not stable in the form of trigonal bipyramide and have symmetry C_{4v} owing to a specific hybridization of d-f-orbitals.

Data on charge-density distribution (charges on atoms, population of valent orbitals, overlap population /OP/, density of state data) as well as energetic characteristics have been obtained as a result of calculations. In Fig.1 we present the outer electron structure for the pentahalides of the group V elements. In table 1 the electron density distribution data are given.

Table 1

Charges on atoms(Q) and atomic populations(q) for MCl₅

Molecule	R(M-Cl), Å	Q	q _s	q _p	q _d	OP
VCl ₅	2.19	1.12	0.24	0.36	3.28	1.74
NbCl ₅	2.29	0.92	0.21	0.23	3.65	2.07
TaCl ₅	2.30	0.94	0.37	0.33	3.35	2.52
PaCl ₅	2.44	0.98	0.13	0.13	2.09	1.96
HaCl ₅	2.38	0.79	0.58	0.35	3.27	2.62

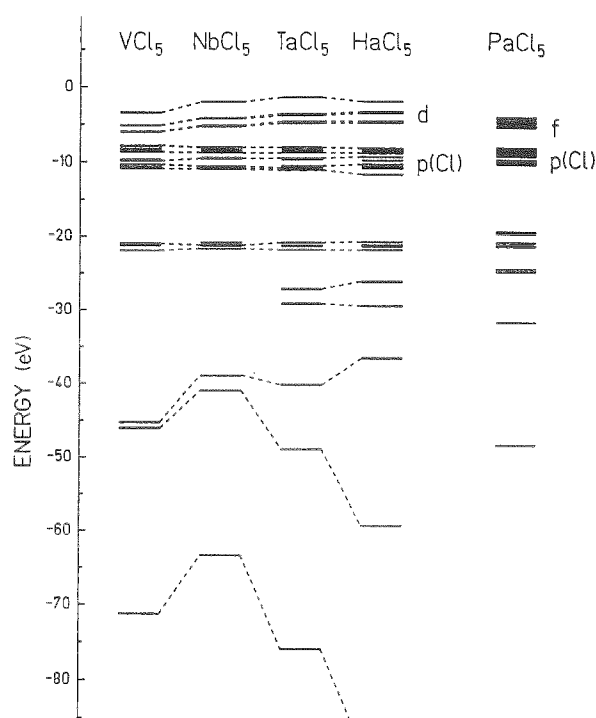
The calculations have shown that the overlap population which is the direct quantitative measure of the covalent bond strength is the smallest in case of VCl₅ and the highly ionic character of this molecule is the reason for its instability. PaCl₅ in its turn cannot be considered as a full analog of the elements of group V owing to the different character of 5f-orbital bonding leading even to a different geometry. Within the three full analogs (Nb, Ta and Ha) the changing of the characteristics is not monotonous and the two constituents of the chemical bond strength are changing in a different way. From Nb to Ta both ionic and covalent contributions are changing in the same

direction giving rise to increase in chemical bond strength while from Ta to Ha the increase in covalent contribution is compensated by decrease in ionic bond order.

To trace the influence of relativistic effects on the nature of chemical bonding in heavy systems we analyzed the overlap populations separately between all valent spin-orbitals. The results have shown that relativistic stabilization of 6p_{1/2}-orbitals and strong destabilization of 6p_{3/2}-orbitals in case of hahnium halides result in total overlap between p-orbitals and valent ligand orbitals being intermediate between Nb and Ta.

Energy equivalent of the overlap population plus ionic bond order plus energy of ionic-covalent resonance give the final value of dissociation energy characterizing the chemical bond strength. Improvements made in total energy calculations⁴ combined with 'counterpoise' scheme let us estimate dissociation energies to be similar for TaCl₅ and HaCl₅.

The volatility of chemical compounds is a complicated process influenced mainly by the nature of intermolecular interaction in the solid state. So the small ionic constituent and rather big covalent one for hahnium halides compared to its analogs give strong reason to believe that volatility of pure HaCl₅ and HaBr₅ should be higher than those of Nb and Ta or close to Ta.

Fig.1: Energy eigenvalues of the outer electrons for MCl₅

1. Gäggeler H.W., Jost D.T., Baltensperger U. et al., "First Results from Gaschemistry Experiments with Hahnium", PSI-Bericht Nr.49, November 1989
2. Schädel M. "Radiochemical studies of the transactinide elements", GSI-89-72 Preprint, October 1989
3. Rosen A. et al., J.Chem.Phys., 62, 3039 (1975)
4. Kolb D., Bastug T. Contributions to the work

G
Subthreshold Production of Hypernuclei at SIS: Status of Preparations

T. Krogulski, W. Brüche, H. Folger, S. Polikanov, M. Schädel, K. Sümmerer, G. Wirth

GSI Darmstadt

E. Stiel, T. Aumann, J.V. Kratz, K. Lützenkirchen, N. Trautmann

Institut für Kernchemie, Universität Mainz

A set of low-pressure, MPWC counters, foreseen to work in a START-STOP mode for two-dimensional position identification, were installed and the linearity of their response signals was tested. Integral and differential linearity was measured. For signal processing an electronic hardware set-up was designed and coupled to serve the DAQ system based on a CAMAC single crate system, operating under GOOSY control. Three options for a hardware main trigger are available: (i) single counter hit trigger, (ii) single track (start-stop) trigger, and (iii) two tracks-in-coincidence trigger. Integral and differential linearity of time to digital and pulse height to digital converters were measured; calibration constants for channels to time units conversion defined.

An analysis programme for a GOOSY environment was developed. To be a virtually on/off line programme, it will contain three layers of subroutines for (i) measurement monitoring, (ii) testing, and (iii) data evaluation.

A first off-line simulation of an experiment was performed with a 4π type ^{252}Cf fission source. A scheme of the experimental set-up is given in a companion report by E. Stiel et al., and an example of one type of monitoring spectra is presented in fig.1.

The aim of this simulation measurement was:

- a) to test the performance of the complete experimental set-up,
- b) to get calibration constants for units conversion: channels to millimeters and nanoseconds,
- c) to get calibration constants (off-sets) to localize space and time coordinate system, in which an event (an ensemble of tracks and vertexes) is described, and
- d) to get a quantitative estimate of the precision with which space and time reconstruction of events can be accomplished.

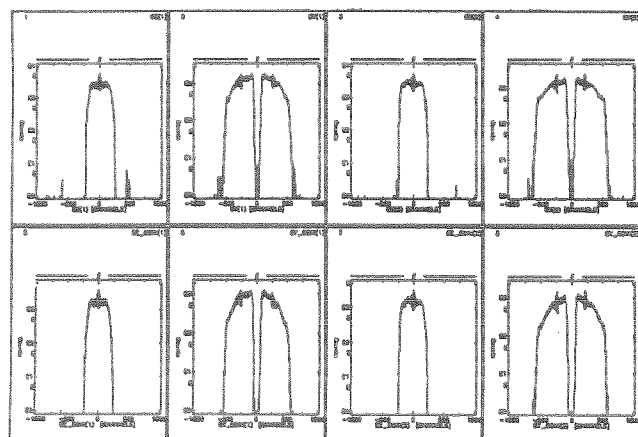


Fig.1: Distributions of hit points in START-counters. Top row-single mode; bottom row-coincidence mode.

Such an estimation was made by comparing: 1) two-dimensional plots obtained from the measured distributions of vertexes with the well known dimensions of our ^{252}Cf source, and 2) the reconstructed velocity distributions of fission fragments with literature data.

Points a), b) and c) are fulfilled; evaluation of data needed to complete point d) is under way.

A qualitative illustration of the performance of our detection system is given in fig. 2: bi-dimensional distribution of TOF signals versus dE/dx signals for fission fragments from ^{252}Cf spontaneous fission, detected in a complete experimental arrangement.

For a few hours a gold target, 0.2 mm thick and $10 \times 50 \text{ mm}^2$ large, was irradiated with a slowly extracted parasitic beam of 220 MeV/u Ar ions, with an intensity of about $0.5 \times 10^8/\text{sec}$. in a large beam spot of about $20 \times 60 \text{ mm}^2$. Under such conditions virtually no background events were observed in our counters, and altogether ~ 600 tracks pointing to the gold target, with TOF and dE/dx signals, characteristics for heavy fragments, were collected.

We are now prepared to measure prompt fission from interactions of relativistic heavy ions with the type of bismuth targets planned to be used for subthreshold hypernuclei production measurements.

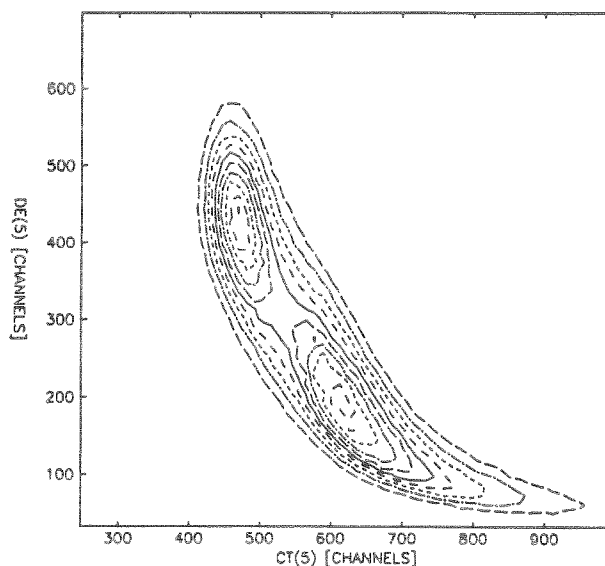


Fig.2: Contour plot of fission events displayed in coordinates: TOF x dE/dx .

Detector and Beam Diagnostic Set-up Inside the USCHI Chamber^G

E.Stiel, T.Aumann, J.V.Kratz, K.Lützenkirchen, C.Sastri
 Institut für Kernchemie, Universität Mainz

K.H.Behr, W.Brüchle, H.Folger, E.Jäger, T.Krogulski, S.Polikanov, M.Schädel, E.Schimpf, G.Wirth
 Gesellschaft für Schwerionenforschung mbH, Darmstadt

The recently modified scattering chamber USCHI¹ is now available in the High-Dose Multi Purpose (HDMP) cave. Various kinds of beam entrance and exit windows, e.g. 0.45 mm thick stainless steel or 25 μm thick KaptonTM foils, allow to run experiments under atmospheric conditions totally independent from the high vacuum requirements of the SIS.

As a preparation for an experiment to search for hypernuclei² six multi-wire proportional counters (MWPC)³ are mounted on a removable platform. A symmetrical set-up on either side of the beam axis was arranged such that time and position signals can be obtained from one START and two STOP detectors, see Fig 1. They allow not only a time-of-flight (TOF) measurement but also the reconstruction of the vertexes for the detected reaction products. The STOP counters provide also pulses depending in the specific ionisation dE/dx of the penetrating particles. This information used together with TOF data allow for an approximate identification of distributions of the mass A and the atomic number Z of the detected reaction products.

Gas Pressure Control Units (GPCU), using piezo electric sensors inside the chamber, maintain a constant heptane vapour pressure of 2.2 ± 0.1 Torr in the MWPCs. Additional safety features like automatic by-pass valves, connecting the gas supply system with the chamber, are implemented. This set-up has allowed to run the detectors for three weeks without any supervision.

A precisely positioned, adjustable aluminum frame with the inner dimensions of $170 \times 80 \times 135$ mm², located in the center between the two START detectors, serves as a multipurpose support for various kinds of target holders and/or detectors. It is movable between a sluice¹ and the main chamber, via a remote control. For the hypernuclei experiment² 6.7 mg/cm² thick titanium stripes of 42.5×2.5 mm² will be used as target backings. They can easily be handled and mounted in a holder to obtain a good planarity. It is thick enough to stop all fission fragments and will serve to create a shadow in the backward hemisphere. Bismuth, 150 $\mu\text{g}/\text{cm}^2$ in the search for Λ -hypernuclei and 800 $\mu\text{g}/\text{cm}^2$ for prompt fission studies, has been evaporated onto the backing to form a target spot of 10×2.3 mm². A target box carrying a stack of upto 12 targets together with sets of absorbers to stop prompt fission products can be inserted in the frame mentioned above; see Fig 2. Presently the beam can be monitored inside the chamber using three independent devices which can remotely be moved in and out of the beam. A set of four scintillators with a size of $50 \times 10 \times 5$ mm³ are arranged in adjustable holders as two pairs in such a way that two are in a vertical and two are in horizontal position. With an opening of presently 10 mm between the two scintillators of each pair they can either serve to monitor the beam halo or to find best conditions while tuning the beam onto the target. A 45×45 mm² thin aluminum plate with 30 mg/cm² LumiluxTM Grün RGS (Riedel-de Haën) serves as a luminous screen and is monitored with a small video camera (CCD Monochrome Image Module, Philips Valvo) mounted inside the vacuum chamber. In a first test with 220 MeV/u ⁴⁰Ar an elliptic beam spot of $\sim 20 \times 50$ mm² was clearly visible at an intensity of about 10^6 ions per spill (600 ms). A third monitoring part is a CCD-video-chip which should be exposed directly to the beam. This equipment was not yet tested since a beam well focused to a spot of some millimeters is presently not available at the HDMP

cave. A video digitizer together with an Amiga 2000TM computer is able to transform the video signals from the camera or the CCD-chip into a picture with 32 colours related to the brightness in the original black-and-white picture. The digitizer can run with an external trigger e.g. from the accelerator. The program provides several options to control in the interactive way the positioning and focusing of the beam.

¹ E.Schimpf et al. , GSI Scientific Report 1989, GSI 90-1, p.262

² T.Krogulski al. , contribution to this report

³ A.Breskin et al. , Nucl. Instr. Meth. 217 (1983) 107

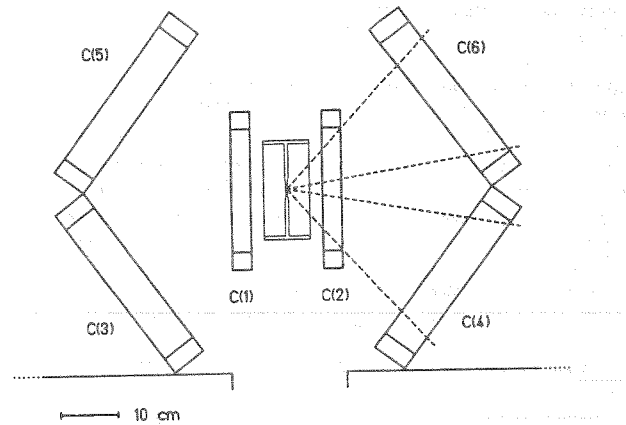


Fig.1: Schematic view in beam direction of the detector set-up with the two START C(1) + C(2) and the four STOP detectors C(3) — C(4). The target box is indicated together with the holder of a target. The dashed lines mark the opening angles for the STOP counters.

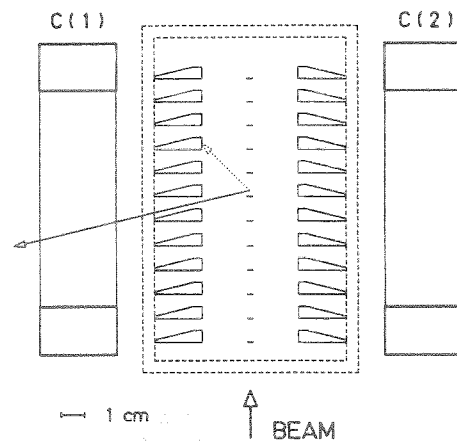


Fig.2: Top view of the two start counters C(1) + C(2) with an arrangement of twelve targets and the corresponding absorbers. The detectors, shielded in forward angles (dashed line arrow), are illuminated in backward angles (solid line arrow) from delayed fission process located at a position downstream the target.